

# WE'VE GOT YOUR SOLUTION

**KILLS TB IN 1 MINUTE**

## Tristel™ DUO DISINFECTANT

### Fast-acting, cost-effective

Tristel DUO is designed to provide fast-acting and cost-effective cleaning and disinfection for instruments and non-critical medical devices including ultrasound transducers, holders, cables, keyboards, and ultrasound stations. With a maximum kill time of 2 minutes for bacteria and a minimum time of just 1 minute for tuberculosis and fungi, Tristel DUO really packs a punch. Tested and proven effective against HPV<sup>1</sup>, Tristel DUO bridges the gap where low-level disinfection is insufficient and high-level disinfection is unnecessary.

**ALCOHOL FREE • BLEACH FREE**

### The Power is in the Process

- Patented dispensing system generates the active ingredient – chlorine dioxide (ClO<sub>2</sub>).
- ClO<sub>2</sub> destroys pathogens by separating electrons from microorganisms' vital structures resulting in molecular imbalance and microorganism death.
- Simply dispense, apply, and allow to dry. Use with any dry wipe.



*Tristel DUO is manufactured and marketed in the United States by Parker Laboratories, Inc. as licensed by Tristel.*

1. Meyers C, Milici J, Robison R. The ability of two chlorine dioxide chemistries to inactivate human papillomavirus-contaminated endocavitary ultrasound probes and nasendoscopes. J Med Virol. 2020 Aug;92(8):1298-1302. doi: 10.1002/jmv.25666. Epub 2020 Feb 4. PMID: 31919857; PMCID: PMC7497195.



Parker Laboratories, Inc.


The sound choice in patient care.™


973.276.9500

parkerlabs.com

# The Ultrasound Window Into Vascular Ageing

A Technology Review by the VascAgeNet COST Action

Elisabetta Bianchini, PhD, MSc , Andrea Guala, PhD, MSc, Spyretta Golemati, PhD, Jordi Alastruey, PhD, Rachel E. Climie, PhD, Kalliopi Dalakleidi, PhD, MSc, Martina Francesconi, PhD, MSc, Dieter Fuchs, PhD, Yvonne Hartman, PhD, Afrah E.F. Malik, MSc, Monika Makūnaitė, PhD, Konstantina S. Nikita, MEng, MD, PhD, Chloe Park, PhD, Christopher J. A. Pugh, PhD, Agnė Šatrauskienė, MD, Dimitrios Terentes-Printizios, PhD, MD, Alexandra Teynor, PhD, Dick Thijssen, PhD, Arno Schmidt-Trucksäss, MD, MA, Jūratė Zupkauskienė, MD, Pierre Boutouyrie, MD, PhD, Rosa Maria Bruno, MD, PhD, Koen D. Reesink, PhD

 Supplemental material online at [ultrasoundmed.org](http://ultrasoundmed.org)

Received November 28, 2022, from the Institute of Clinical Physiology, CNR, Pisa, Italy (E.B., M.F.); Vall d'Hebron Institut de Recerca (VHIR), Barcelona, Spain (A.G.); CIBERCV, Instituto de Salud Carlos III, Madrid, Spain (A.G.); Medical School, National and Kapodistrian University of Athens, Athens, Greece (S.G.); Department of Biomedical Engineering, King's College London, London, UK (J.A.); Menzies Institute for Medical Research, University of Tasmania, Hobart, Tasmania, Australia (R.E.C.); INSERM, U970, Paris Cardiovascular Research Center (PARCC), Université de Paris, Hôpital Européen Georges Pompidou - APHP, Paris, France (R.E.C., P.B., R.M.B.); Biomedical Simulations and Imaging (BIOSIM) Laboratory, School of Electrical and Computer Engineering, National Technical University of Athens, Athens, Greece (K.D., K.S.N.); University of Pisa, Pisa, Italy (M.F.); Fujifilm VisualSonics, Amsterdam, The Netherlands (D.F.); Department of Physiology, Radboud Institute for Health Sciences, Radboud University Medical Center, Nijmegen, The Netherlands (Y.H., D.T.); CARIM School for Cardiovascular Diseases and Heart and Vascular Center, Maastricht University Medical Center+, Maastricht, The Netherlands (A.E.M., K.D.R.); Biomedical Engineering Institute, Kaunas University of Technology, Kaunas, Lithuania (M.M.); MRC Unit for Lifelong Health and Ageing, University College London, London, UK (C.P.); Cardiff School of Sport & Health Sciences, Cardiff Metropolitan University, Cardiff, UK (C.J.A.P.); Clinic of Cardiac and Vascular Diseases, Institute of Clinical Medicine, Faculty of Medicine, Vilnius University, Vilnius, Lithuania (A.Š., J.Z.); Centre of Cardiology and Angiology, Vilnius University Hospital Santaros klinikos, Vilnius, Lithuania (A.Š.); First Department of Cardiology, Hippokraton Hospital, Medical School, National and Kapodistrian University of Athens, Athens, Greece (D.T.-P.); Faculty of Computer Science, Augsburg University of Applied Sciences, Augsburg, Germany (A.T.); and Department of Sport, Exercise and Health, Division Sport and Exercise Medicine, University of Basel, Basel, Switzerland (A.S.-T.). Manuscript accepted for publication April 14, 2023.

Elisabetta Bianchini is co-founder of Qipu srl (Pisa, Italy), a spin-off company of the Italian National Research Council and the University of Pisa. Dieter Fuchs is employed by Fujifilm VisualSonics. The other authors declare no competing interests.

Address correspondence to Elisabetta Bianchini, Institute of Clinical Physiology, CNR, Pisa, Italy.

E-mail: [elisabetta.bianchini@ipc.cnr.it](mailto:elisabetta.bianchini@ipc.cnr.it)

## Abbreviations

AP, atherosclerotic plaque; ARFI, acoustic radiation force impulse; CAR, carotid artery reactivity; CCA, common carotid artery; CEUS, contrast-enhanced US; CPT, cold pressor test; CVs, coefficients of variation; EDV, end-diastolic velocity; FMD, flow mediated dilation; fps, frames per second; GSM, gray scale median; H-FMC, high-flow mediated constriction; IM, intima-media; IMR, intima-media roughness; IMT, intima-media thickness; L-FMC, low flow-mediated constriction; PAI, photoacoustic imaging; PI, pulsatility index; PSV, peak systolic velocity; PWI, pulse wave imaging; RF, radiofrequency; RI, resistive index; ROI, region of interest; UHF, ultra-high frequency; US, ultrasound; VAR, vasoactive range; WIA, wave intensity analysis; WSS, wall shear stress

doi:10.1002/jum.16243

This is an open access article under the terms of the [Creative Commons Attribution-NonCommercial-NoDerivs License](https://creativecommons.org/licenses/by-nc/4.0/), which permits use and distribution in any medium, provided the original work is properly cited, the use is non-commercial and no modifications or adaptations are made.

Non-invasive ultrasound (US) imaging enables the assessment of the properties of superficial blood vessels. Various modes can be used for vascular characteristics analysis, ranging from radiofrequency (RF) data, Doppler- and standard B/M-mode imaging, to more recent ultra-high frequency and ultrafast techniques. The aim of the present work was to provide an overview of the current state-of-the-art non-invasive US technologies and corresponding vascular ageing characteristics from a technological perspective. Following an introduction about the basic concepts of the US technique, the characteristics considered in this review are clustered into: 1) vessel wall structure; 2) dynamic elastic properties, and 3) reactive vessel properties. The overview shows that ultrasound is a versatile, non-invasive, and safe imaging technique that can be adopted for obtaining information about function, structure, and reactivity in superficial arteries. The most suitable setting for a specific application must be selected according to spatial and temporal resolution requirements. The usefulness of standardization in the validation process and performance metric adoption emerges. Computer-based techniques should always be preferred to manual measures, as long as the algorithms and learning procedures are transparent and well described, and the performance leads to better results. Identification of a minimal clinically important difference is a crucial point for drawing conclusions regarding robustness of the techniques and for the translation into practice of any biomarker.

**Key Words**—arteriosclerosis; atherosclerosis; ultrasound; vascular ageing

## Introduction

Ultrasound (US) imaging enables the assessment of both structural and functional properties of superficial blood vessels.<sup>1,2</sup> Most of the available evidence relates to the carotid artery, a large central artery, which has been shown to reflect morphological and functional aspects of the arterial tree that are relevant to (early) disease detection and monitoring.<sup>3–7</sup> Other arterial segments such as the femoral, brachial, or aortic segments accessible by US have also been considered in epidemiological and pharmacological research to improve cardiovascular risk prediction and to investigate vascular effects of cardiovascular drugs.<sup>8–10</sup>

Over the past four decades, major technological developments have spawned the exploration, validation, and use of multiple vascular diagnostics and characteristics in clinical, as well as interventional and

epidemiological, study settings. Today, the paradigm in vascular medicine is shifting from primary/secondary prevention toward global management of vascular health in a life course perspective.<sup>9</sup> In this context,

**Figure 1.** Vascular ageing parameters considered in this review. CAR, carotid reactivity; FMD, flow-mediated dilation; IMT, intima-media thickness.

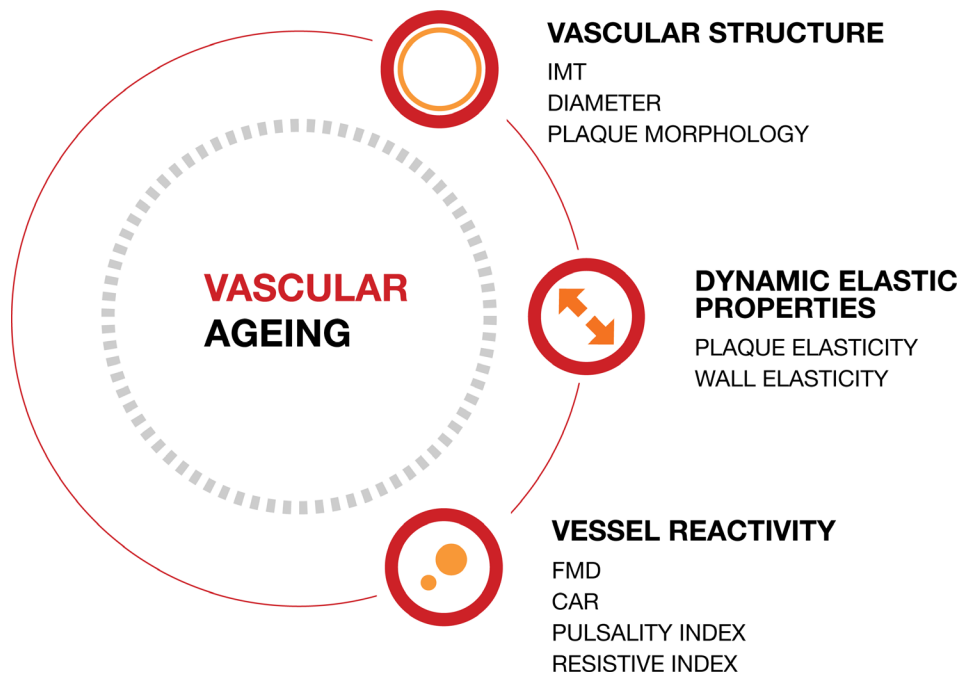
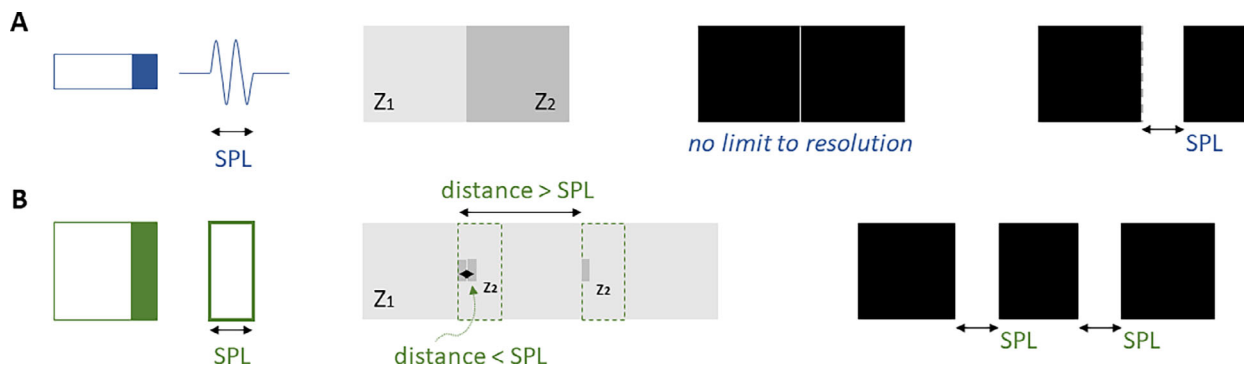


**Figure 2.** Resolution poses a lower limit to discriminate objects by imaging. **A**, in case of echography, the idealized location of an ideal boundary between two homogenous media with differing acoustic impedances  $Z_1$  and  $Z_2$  yields a thin line in a black background. However, the boundary is typically reconstructed as a wider line due to the real emitted spatial pulse length (SPL). Note that here, still an idealized case is assumed in which only the emitted SPL determines resolution. **B**, Illustration showing that two reflective objects spaced apart less than the axial resolution cannot be distinguished, or “resolved.” When the spacing exceeds the resolution, the reflective objects can be resolved. A greater bandwidth (which is determined by the emission frequency and quality factor  $Q$  of a transducer) reduce SPL and will thus improve axial resolution. Here, pure reflection is assumed (no scattering), hence the B-mode image is binary (black-and-white).



vascular ageing is seen as an inevitable but modifiable process driving the more overt manifestations of cardiovascular disease, and usually depicted by two different phenomena: arteriosclerosis and atherosclerosis.<sup>11</sup> The vascular ageing process occurs as part of normal, physiological ageing, with large interindividual differences, related both to individual susceptibility and exposure to environmental and behavioral factors. An example is provided by individuals whose arteries appear abnormally healthy in comparison to their cardiovascular risk factor burden representing a studied model to find effective approaches for cardiovascular protection.<sup>12</sup> Mechanisms underlying this phenomenon are not fully understood, thus direct assessment of vascular status is crucial for correct evaluation of vascular ageing.<sup>12,13</sup> Accordingly, personalized assessment of vascular ageing could take a central role in health management, both at an individual and population level. US imaging offers versatility, affordability, and accessibility to match the practical conditions and economic constraints around health management.

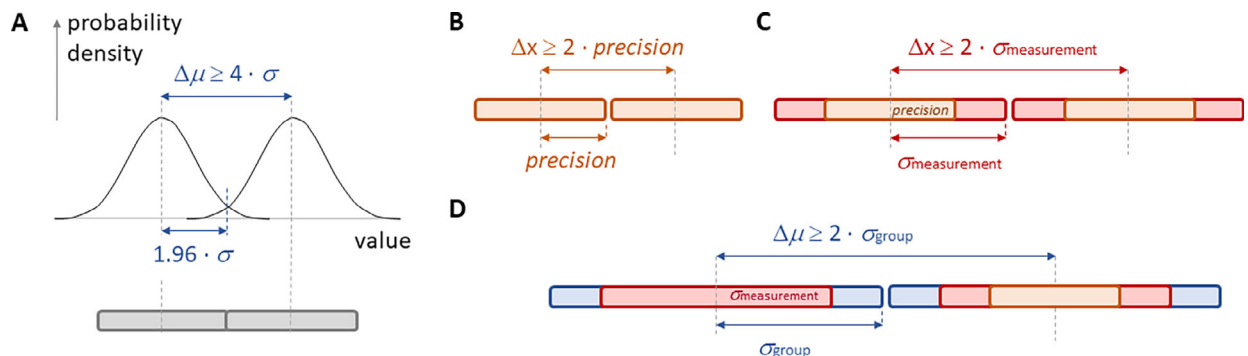
The purpose of the present article was to review the current state-of-the-art non-invasive US technologies and their ability to capture vascular age-related changes from a technological perspective. Following an introduction on the basic concepts of the US technique, the characteristics considered in this review are clustered into: 1)

vessel wall structure; 2) dynamic elastic properties, and 3) reactive vessel properties, as summarized in Figure 1. Since *precision* (ie, repeatability/reproducibility) and *accuracy* (ie, closeness to real value)<sup>14</sup> determine the best-possible performance of a marker in practice, our literature search particularly focused on performance in terms of these measures, taking into account that resolution of the technique poses initial limits (Figures 2 and 3). It should be noted that no single final number will capture precision or accuracy of the vascular ageing literature, since the system, mode, settings, or conditions are different for the different parameters.

### METHODOLOGY (WRITING AND EDITING PROCESS)

This review was conceived within the VascAgeNet—Network for Research in Vascular Aging, COST Action CA18216 (<https://vascagenet.eu/>)—as an initiative of the Working Group dedicated to harmonization of technologies (WG3).<sup>15</sup> A multidisciplinary subgroup with experience in US imaging was created and the first task was to review the US technology available for assessing vascular ageing. Non-invasive vascular US measurements used in humans<sup>11</sup> and their backgrounds were identified by the whole team

**Figure 3.** Sources of uncertainty. **A.** Statistical principle for detecting difference in a measure ( $\Delta\mu$ ), where a difference of about four standard deviations ( $\sigma$ ) is considered statistically significant in case of normal distributions (as shown). Underneath the distribution curves is a simplified depiction of the limit for detecting a difference (or changes in case sequential measurements are considered). **B.** A first minimal detection threshold for a measurement ( $\Delta x$ ) is primarily determined by the technology/principle/processing-chain used (here characterized by  $\sigma$  system). **C.** In practice, the application of the technology involves multiple sources of uncertainty increasing measurement variability (here characterized by  $\sigma$  measurement): these may involve, for example, intra- and inter-operator variability pertaining to practical conditions and constraints. In **D.**, the ultimate build-up of uncertainty is illustrated for a typical two-group or paired comparative study, showing how various source of variabilities (taken together yield  $\sigma$  group) pose limits to detecting the difference  $\Delta\mu$ .



and members were assigned responsibility, based on expertise, for literature search and selection focused on technical performance of one or more specific vascular topics. The adopted databases were PubMed, Scopus, and Web of Science: key words included the “vascular parameter/technique” and ultrasound and precision/reproducibility/repeatability/accuracy/validation (see online supplemental Data S1). Within this phase other pertinent papers that the authors were aware of or references within the found literature were also considered. The contributions were critically revised by a core group of facilitators (EB, RMB, AG,

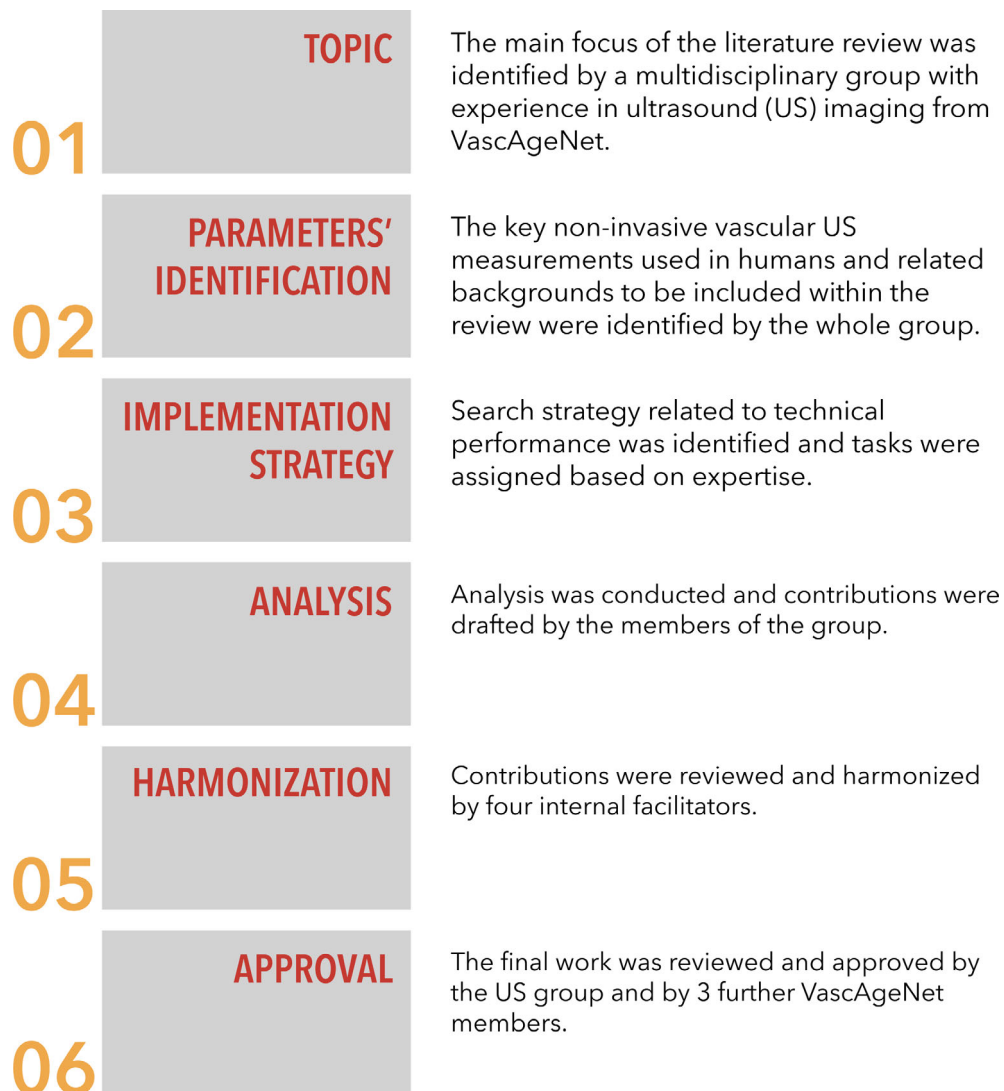
KR), who harmonized the whole manuscript and solved the conflicts by consensus. The final manuscript was then approved by the whole subgroup. As a final step the paper was internally reviewed by three VascAgeNet members (Figure 4).

## Imaging Principles and Operation Modes

### *Physical Principles*

US is a portable, affordable, and safe imaging technique based on the generation of inaudible high-frequency

**Figure 4.** Main steps of the literature review implementation.



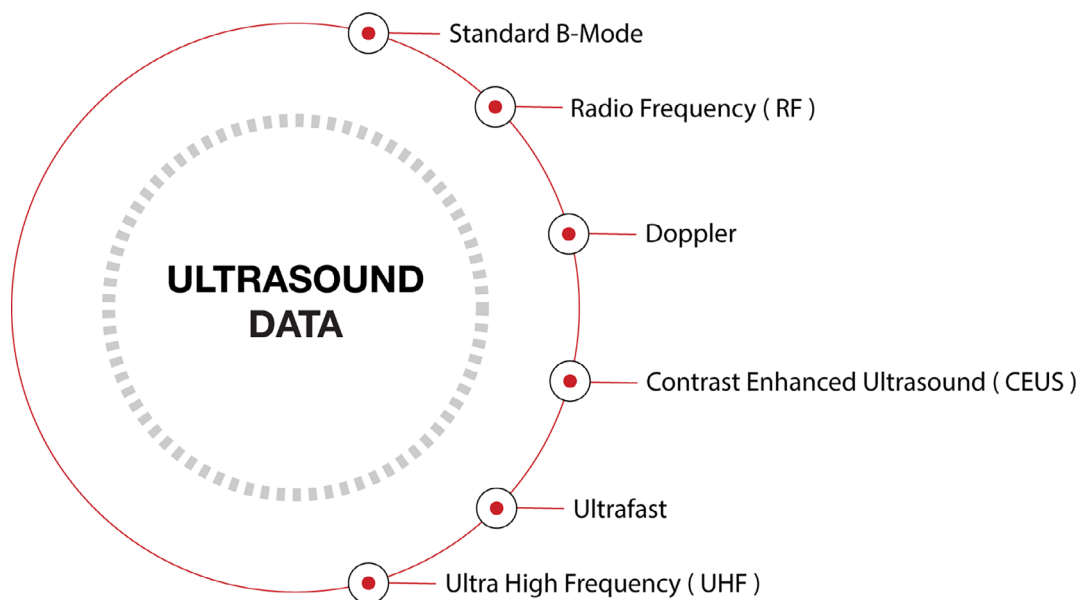
sound waves, their propagation, and the analysis of their reflection and scattering by the imaged tissues.

Longitudinal compression waves are generated by a piezoelectric crystal, which transforms electric signals into deformation and is often called a transducer. An alternating voltage is applied to the crystal that deforms accordingly, producing compression/rarefaction sound waves with the same frequency of the electric signal imposed. In contrast, for wave detection, the opposite happens: the crystal responds to returning sound waves by producing electric signals, which is called radiofrequency (RF) signal. Several characteristics define a RF signal. The wavelength is the distance over which the wave's shape repeats. The maximum pressure fluctuation is called amplitude, while bandwidth is the range of frequencies a transducer can generate. According to the classic wave propagation theory waves propagate in a straight line inside a medium at a specific velocity that remains uniform if the medium is homogeneous. Waves are partially reflected at the interface between heterogeneous medium due to differences in acoustic impedance. These reflected waves travel back to the transducer and are converted into RF signals. The time difference between peaks provides information about the localization of boundaries between

structures. A variety of transducers exist for different applications, the shape, the number of elements, and the central frequency (the lower the frequency the greater the penetration depth but lesser the resolution) are adapted to specific organs. In addition, contrast agents consisting of encapsulated microbubbles containing gases can be used in vascular imaging (for example, for plaque analysis).<sup>16</sup>

US versatility enables the measurement and estimation of a considerable range of vascular characteristics: from the evaluation of structural alterations of arterial layers and composition, to the analysis of related changes in the elastic and reactive properties, for example, to endothelial function or sympathetic activity (Figure 5). Application is limited to superficial sites and due to the availability of different systems, standardization is a crucial aspect. The wide adoption of US in clinics provides a concrete opportunity for the implementation of a safe and relatively low-cost integrated picture based on the vascular characteristics we are describing within this work and positively impacting in the patient's management. Different techniques for US wave generation, working principles and data processing give rise to a variety of different imaging modes. More specifically, core US data used in vascular health assessment are: motion (M-)

**Figure 5.** Ultrasound data output that can be obtained non-invasively.



mode and brightness (B-) mode and Doppler signal analysis.

### ***M-Mode and B-Mode***

In most cases cardiovascular structures are visualized via a pulse-echo principle, where the transducer is used in alternation as the generator (pulse) and the receiver (echo). The strength of the echo (proportional to image brightness) and the time between pulse generation and echo return are used together with known propagation velocity to obtain an estimate of axial distance (in different cardiovascular tissues, US wave velocity clusters around an average value of 1540 m/s). If this working structure is repeated over time from a fixed perspective (ie, fixed beam direction), time-resolved one-dimensional M-mode images are obtained. Conversely, if the direction or location of the generated beams varies over time, either manually or more-often, electronically, two-dimensional (2D) or three-dimensional (3D) B-mode (brightness) images are generated. Temporal and spatial resolutions of B-mode images are inter-related and further depend on the size of the imaged sector, the depth of the visualized structure, and the characteristics of the transducer. Spatial resolution is generally depicted in three directions: axial (along the beam direction), lateral (in the image plane perpendicular to the beam direction), and elevational (perpendicular to the imaging plane, also called slice thickness). Because it relies on the balance between the differences in travelling time between two neighboring regions, axial resolution is mainly proportional to the transmitted US pulse length (Figure 2). Shorter pulses can be generated by a higher frequencies transducer thus improving axial resolution. Typically, the frequency of standard vascular US ranges between 7 and 18 MHz, but higher frequencies (46–70 MHz) are increasingly used in vascular ultrasound. Practical resolution typically varies between 300 and 30  $\mu\text{m}$  for normal and high-frequency systems, respectively. Lateral and elevational resolutions are mainly determined by the width of the beam used and they are, in general, one order of magnitude lower than the axial resolution.

In summary, a minimum resolvable sample volume can be defined. This sample volume can be approximately considered as wide and high as half of the beam width at a given location and as deep as half

of the pulse length. Finally, temporal resolution depends on the rate of image generation. In particular, the time US waves take to travel to the target and come back limits the rate at which images can be acquired. Temporal resolution of B-mode images is also inversely related to the number of scan lines. It can be improved by reducing the spatial resolution or the size of the image, simultaneously acquiring multiple sectors, and increasing the frequency bandwidth. As previously mentioned, increasing pulse frequency is beneficial in terms of spatial resolution. However, high frequencies are subjected to larger attenuation, which in turn limits the imaging depth; hence, a compromise must be found. Typical time resolution for US standard equipment ranges between 20 and 60 fps in B-mode and up to 1000 fps in M-mode.

Ultrasound image quality (eg, for enhanced contrast between different regions), can be improved by exploiting multiple sources of information. This is the case for harmonic imaging that uses the harmonics generated from the non-linear propagation of waves through the body tissue.<sup>17</sup> Another approach worth mentioning is compound imaging that combines information from multiple angles of insonation.<sup>18</sup> However, limitations of these approaches can include reduction of temporal resolution due to the time needed for the advanced signal processing.

It is worth mentioning, that raw RF data have been used for the first studies in the field of vessel dimensions and elasticity and the derived echo-tracking devices have been historically considered as the pioneering technique in measuring arterial wall thickness and distension.<sup>6,19</sup> Subsequently, systems that process B-mode output of standard ultrasound equipment, have also been developed.<sup>20–22</sup>

### ***Doppler Signal Analysis***

The other widely applied working principle of US imaging is used to quantify velocities (of blood, heart, and vessels) and relies on the frequency content of the US wave (Doppler Effect). Indeed, moving structures lead to an apparent change in signal frequency resulting from reflection from a target moving in the direction of beam propagation. Several working principles are used for Doppler imaging; they vary with respect to the nature of the generated waves, separating continuous signal (Continuous-wave Doppler) from pulsed signal (pulse-wave Doppler and color

flow Doppler). Continuous-wave Doppler imaging does not distinguish the depth of the velocity, recording all velocities appearing in the beam line, but has no limit on recorded velocity. Conversely, pulse-wave and color flow Doppler allows for the choice of the sampling region, but maximum recorded velocity is limited by the pulse rate frequency (PRF) leading to potential aliasing (Nyquist limit,  $\frac{1}{2}$  of PRF). The maximum measurable velocity is inversely related to the depth of the imaged segment and the PRF. As spatial and velocity resolution of pulse-wave and color flow Doppler are inversely proportional a compromise should be obtained, which normally results in limited spatial resolution.

For both comprehensive and detailed overviews, we refer the reader to the following sources: Refs. [23–25].

Considering that resolution is a determinant of how well a vascular ultrasound characteristic can capture underlying ageing-changes, advanced imaging modes, requiring further technologies and data processing, have been developed.

1. Ultra-high frequency (UHF) US is a relatively new diagnostic imaging technique originally developed for imaging small animals in preclinical research.<sup>26,27</sup> Based on the same physical principles of standard ultrasound, but with frequencies of up to 70 MHz, UHF US has limited penetration depth but can provide an image quality with an axial resolution down to 30  $\mu\text{m}$  (better than standard equipments) and has been used for superficial vascular imaging in

humans (Figure 6) such as radial, tibial, dorsal pedal, temporal, and common carotid arteries.

2. Ultrafast US imaging produces imaging frame-rates up to 10,000 frames per second (fps). Ultrafast US can be used for local arterial stiffness estimation by shear wave elastography and pulse wave velocity along a short arterial pathway, providing a blood pressure-independent estimation.<sup>28</sup> Owing to such an extremely high temporal resolution, ultrafast US imaging enables visualization of rapid dynamic responses of biological tissues. On the other hand, lateral spatial resolution and contrast are inherently worse than that in conventional imaging; vessel elastography can be further limited by inherent tissue motion (Box 1).

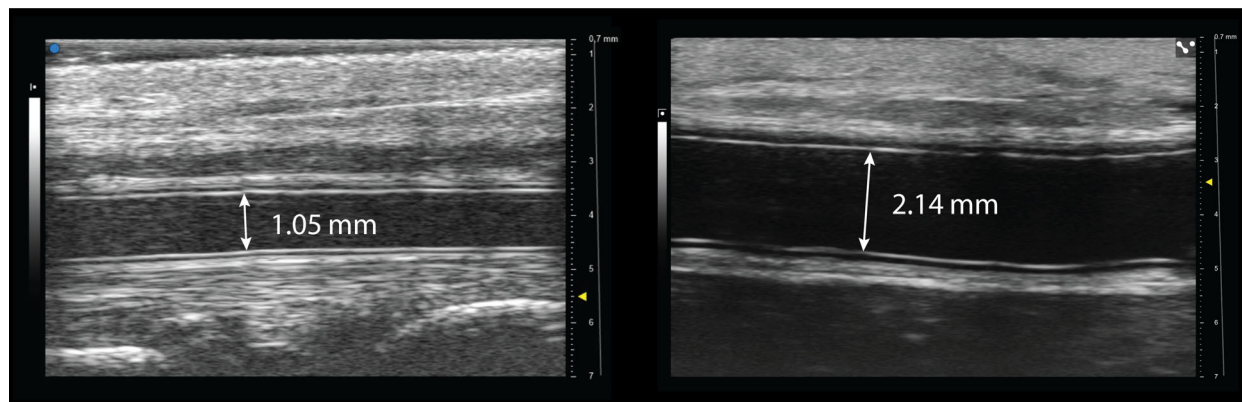
## Reliability and Validity of US Vascular Characteristics

*Resolution*, the capacity to separate two interfaces to be imaged, poses the first limit of what can be

### Box 1. Summary statement

*Ultrasound data:* Different US modes can be used for vascular characteristics analysis, ranging from RF-data, Doppler and standard B/M-mode imaging, to more recent UHF and ultrafast techniques. The most suitable setting for a specific application should be selected according to requirements in terms of spatial and temporal resolutions.

**Figure 6.** Example of Ultra-High-Frequency B-mode imaging: dorsal pedal artery (left) and radial artery (right), scanned with 70 and 50 MHz linear probe, respectively.





observed and, as mentioned above, is related to the specific features of the ultrasound transmitted and the received echo signal (Figure 2). From the derived imaging, several parameters can be estimated. Validity of these parameters in terms of agreement with the true measurement, the so-called *accuracy*, is not always easy to determine, especially when the identification of the gold-standard technique is not univocal. Phantoms represent one option to be used for such quantification, however, in-vivo alternatives, such as manual assessment by a skilled operator are closer to the real practice, and, hence, they are also adopted. Histology may also constitute a reference technique, especially for tissue characterization, but tissue alterations during the process of fixation often modify geometrical characteristics such as wall thickness/diameters. Measurements by RF-based echo-tracking devices<sup>19</sup> have been historically used as the reference value for intima-media thickness (IMT) and instantaneous diameter changes. Raw RF data are not influenced by further post-processing that is implemented in commercial US equipment. These steps are utilized to improve the B-mode image visualization, however, they can affect, for example, the sharpness of interfaces and thus dimensions obtained by edge-detection algorithms that are sensitive to non-linear processing.<sup>29</sup> Similarly, lumen diameter and arterial wall thickness measurements can be altered by US settings, such as dynamic range and gain.<sup>30</sup> Since ultrasound setup can significantly affect vascular parameter assessment, it should be reported and replicated in follow-up scans. Of course, non-linear and non-ideal scattering and reflections in the tissue cannot be circumvented, also not by RF analysis.

Measurement *variability* (ie, precision) might be determined by various sources<sup>22,31</sup> (Figure 3), ranging from data processing<sup>29</sup> to practical conditions such as US equipment setup,<sup>32</sup> type of analysis (manual or automated),<sup>20</sup> subject- and operator-related factors,<sup>21</sup> and heterogeneous vascular anatomy.<sup>22</sup>

Since the US equipment setup has an impact on the final data, B-mode based systems<sup>29,30,32</sup> should be standardized, or at least documented, for follow-up analysis. Protocol standardization, as well as operator training, assist in mitigating subject- and operator-related variability, such as projection of the scans or season, hour of the day, environmental temperature,

menstrual cycle, and so on. This is even more important for reactivity tests (see Section 5.3.1). Data regarding short- and long-term variability are useful to properly estimate physiological variation and for lowering inter/intra-session and inter-/intraobserver variabilities.<sup>33</sup>

When adopting new generation systems, it is important to verify whether values obtained with newer apparatus are comparable to those obtained with older ones. This holds true even for those considered as reference techniques, such as first and last generation RF-based systems.<sup>34</sup> Agreement between different systems and the derived interchangeability must be considered for follow-up studies and when determining reference values.<sup>7,8,35</sup>

For processing US data, algorithms are generally preferred over manual processing since they are time efficient, result in reduced operator dependency and enhanced performance. For example, computer-based arterial wall segmentation methods increase the performance of US carotid artery imaging.<sup>22</sup> It is also interesting to note that the adopted mathematical operator may also introduce small biases, as previously observed for diameter measurements with edge detection methods converging to slightly different points.<sup>36</sup> Recent advances in the field of artificial intelligence have boosted various techniques, for example, for pattern recognition. In particular, the classification of tissue types and the segmentation of distinct structures in medical images might benefit from the application of deep neural networks.<sup>37</sup> New systems for diameter and IMT measurement, offering a higher grade of automation, have recently been proposed<sup>38–41</sup> and tested with respect to a “ground truth.” While in semi-automatic systems, only the detection of the different interfaces is automated, new approaches aim at automating the entire process (detection of the vessel itself, the appropriate selection of the region of interest [ROI], delineation of the interfaces) with the end goal of improving the usability of the final system. Due to the higher computational power of existing computer systems, larger amounts of data can now be used to train these algorithms and to obtain powerful detection systems, besides identifying vessel structure.<sup>42</sup> AI-based approaches might be applied to ultrasound data also for Radiomic features extraction for

instance for plaque characterization.<sup>43</sup> This direction might provide a huge step ahead for the role of vascular ageing assessment, especially if applied to data that can be obtained by low-cost, portable, and safe ultrasound equipment (Box 2).

## Ultrasound-Derived Vascular Characteristics

Vascular characteristics obtainable by US were grouped according to: 1) vessel wall structure, 2) dynamic elastic properties, and 3) reactive vessel properties. Each characteristic is briefly described, including current and emerging approaches, and its reliability and potential impact are reported with a focus on technical performance and ability of the measurement to capture ageing-related changes in vascular properties. An overview of the reviewed literature, and in particular on the performance of the described approaches, is given and more details can be found in Table 3a, 4a, and 5a (reporting accuracy data) and Table 3b, 4b, and 5b (reporting precision data) of online supplemental Data S1. More specifically, the reported accuracy data are related to closeness with the true value, whereas the included precision data are related to repeatability of the measurement. Finally, a summary of strengths and weaknesses is reported for each characteristic.

### Box 2. Summary statement—Reliability and validity of US vascular characteristics

Resolution poses a lower limit to discriminate objects by imaging. Other key measures to consider are technical accuracy and precision. The gold standard approach varies depending on the measured parameter and true value is not easy to be determined. Measurement variability may be determined by various sources and can be lowered using robust (semi-)automatic algorithms. Automatic detection approaches show a lower variability and operator independence than human tracings and thus are preferable. Raw RF data are historically considered as reference for borders and diameter analysis since they are not influenced by further post-processing that is implemented in commercial US equipment.

## Vessel Wall Structure: Intima-Media Thickness, Plaque Morphology, Diameter

### *Intima-Media Thickness*

#### *Vascular Characteristic*

Intima-media thickness (IMT) corresponds to the thickness of the two innermost layers of the artery wall.<sup>19,44</sup> The adventitia is not included because of difficulties to delineate it precisely. IMT is typically quantified on the far wall of the common carotid artery (CCA), where it is considered more reliable,<sup>45</sup> but can be measured in the internal carotid, femoral, radial, popliteal, brachial arteries, or infrarenal abdominal aorta too.<sup>46,47</sup>

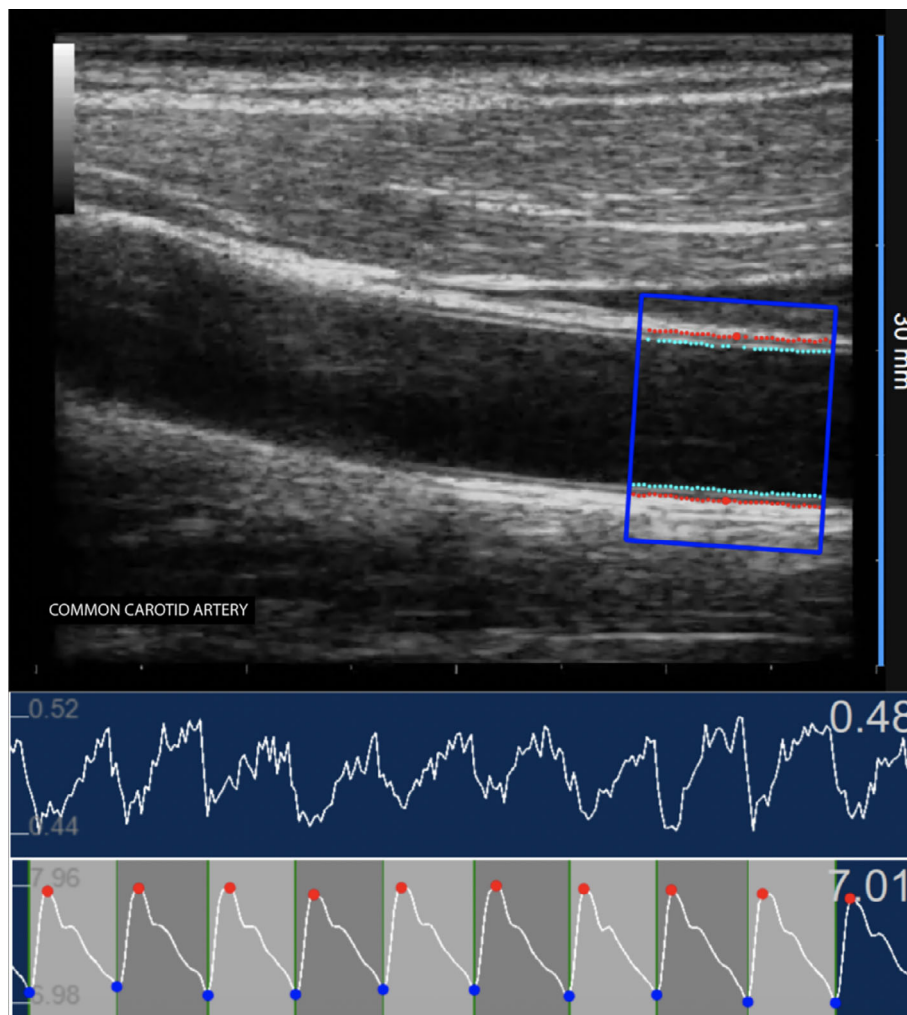
*Technological Approach*—IMT can be assessed based on standard B-mode, UHF B-mode, and RF data. IMT is usually obtained on longitudinal scans with a linear US probe. Originally derived manually, by using the machine calipers on ECG-gated images, the introduction of more recent computerized methods (Figure 7) improved the assessment of IMT thanks to the use of segmentation approaches and can be derived by the spatial average within a ROI and temporal average on several frames.<sup>22</sup> Carotid IMT was first described as a characteristic B mode image composed of two parallel echogenic lines separated by a hypoechoic space by Pignoli et al.<sup>48</sup> The distance between the leading edges of the two parallel lines, corresponding to the two anatomical boundaries, the lumen-intima, and media-adventitia interfaces, corresponds well with IMT measured in histological specimens.<sup>44</sup>

*Future Development and Emerging Approaches*—UHF US has a higher axial resolution for assessing IMT compared with conventional US. Hence, it can be used in the more superficial arteries such as the radial, tibial, dorsal pedal, or temporal artery, and common carotid arteries, especially in children.<sup>49</sup> When muscular arteries such as the radial or temporal artery are insonated by UHF US, additional echogenic lines can be usually seen, with possible promising applications for the measurement of different wall layers.<sup>50,51</sup> Recently, Sundholm et al<sup>52</sup> proposed a standardized method of measuring arterial wall layers in adult temporal arteries, based on the identification of a four-line pattern, showing correlation with histology and

low intra- and interobserver variability.<sup>52</sup> Efforts in standardizing image acquisition and data analysis are currently ongoing. Emerging approaches to study IMT include the analysis of IMT irregularity. This is based on the general principle that atherosclerosis is an inflammation process causing roughness of the intima-media (IM) layer of the arteries and leads to plaque formation.<sup>53</sup> Carotid intima-media roughness (IMR) is calculated as the arithmetic mean of the IMT profile deviation areas from the IMT regression line. Carotid IMR is increased in old compared with young individuals and may correspond to pre-plaque atherosclerotic changes of the arterial wall.<sup>54,55</sup>

*Accuracy.* Works describing the technical accuracy of IMT are mainly performed in the carotid artery. Many semiautomatic B-mode-based systems assessed technical accuracy by agreement (ie, Bland–Altman plots) with semiautomatic RF-based systems or with manual analysis (calipers) by a skilled operator (single or average of several manual measurements)<sup>36,56–60</sup>. It is worth noting that AI-based approaches are generally validated against manual measurement. The reported standard deviation of the differences are tens of  $\mu\text{m}$  (in regard to 0.5–1 mm wall thickness), when comparing two separate acquisitions by two different systems and

**Figure 7.** Example of a contour tracking algorithm applied on B-mode carotid image sequences (top); obtained phasic IMT and diameter waveform measurements [mm] (bottom). The artery was scanned with a 10 MHz linear probe. Image resolution is 15.9 pixel/mm.



slightly lower when analysing the same data. UHF radial and anterior tibial arterial thickness has been tested on silicon phantoms, resulting in a few  $\mu\text{m}$  error.<sup>61</sup>

**Precision.** Most papers reported coefficients of variation (CVs) or intra-class correlation, and comparable data are available for RF and B-mode-based approaches. Some work has evaluated the repeatability of the measurement on the same ultrasound acquisition, whereas others estimate repeatability in a session by removing and repositioning the probe (same operator or two operators) or in different sessions, obtaining a maximum CV of 8% for semi-automatic approaches in the common carotid IMT.<sup>34,36,46,62–64</sup> Femoral, popliteal, and abdominal aorta show slightly higher variability.<sup>46</sup> Dorsal pedal and radial artery thickness precision in UHF US images has been analyzed, and reported to be comparable to conventional B-mode.<sup>51,65</sup> Finally, a recent study compared the head-to-head variability among several manual and algorithm-based systems on the same set of images.<sup>20</sup> Lower CV was reported when considering only the algorithm-based methods (21% vs. 17%).

**Clinical impact.** Common carotid IMT is known to linearly increase with age in both sexes, corresponding to the development of either atherosclerosis at the intimal level or medial hypertrophy.<sup>7</sup> Elevated IMT is considered as an early marker of atherosclerosis. Reference values for common carotid IMT are available and were determined in 24,871 individuals (53% men; age range 15–101 years) using both RF and B-mode based processing techniques.<sup>7</sup> Increased IMT is associated with cardiovascular events,<sup>66</sup> but has no added value for risk stratification on top of classical risk factors.<sup>67,68</sup> However, monitoring IMT changes can be useful as a surrogate endpoint in cardiovascular drug trials.<sup>66</sup>

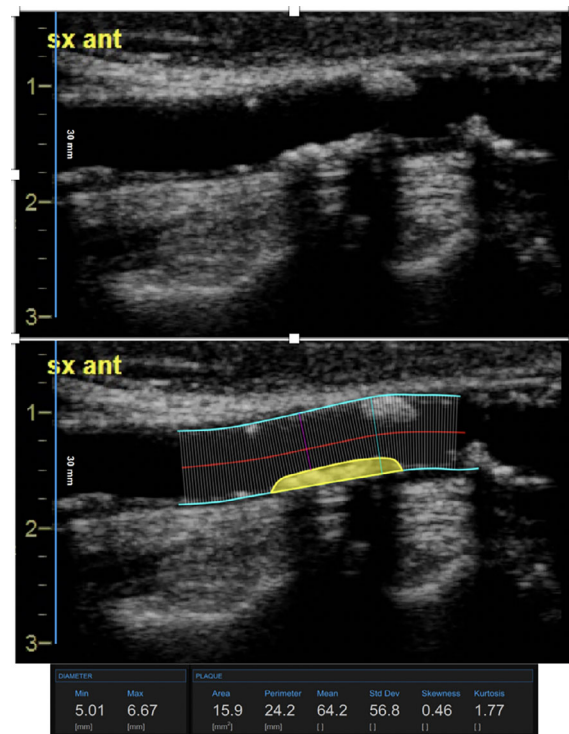
**Strengths and Weaknesses—**The approach is consolidated since 1) semi-automatic systems are available on the market; 2) literature data about the reliability of the measurement in terms of accuracy and precision are widely available; 3) reference values have been provided by the scientific community. The added value of this parameter in patient's management is still controversial.

### Atherosclerotic Plaque

**Vascular Characteristic—**Atherosclerotic plaque (AP) is the main feature of the atherosclerotic process and consists in a focal thickening of the intimal layer of the arterial wall (>50% of the surrounding wall thickness) due to accumulation of lipids, inflammatory and muscular cells, fibrous tissue, and calcium.

**Technological Approach—**In clinics, the plaque is usually evaluated in terms of percentage of stenosis<sup>69</sup> and a detailed analysis is out of the scope of this work. From a tissular perspective, AP can be characterized by a whole image approach and by methods that analyze individual pixels. AP presence and geometry, usually at the carotid and femoral sites, can be assessed with 2D and more recently also with 3D imaging (volume).<sup>70,71</sup> In particular, burden (eg, AP number, involved territories), geometry (size expressed, eg, as area, width, height, see Figure 8) and surface characteristics can be derived. 3D ultrasound has shown

**Figure 8.** Example of plaque morphology measurements. The artery was scanned with a 10 MHz linear probe.



higher plaque burden with increasing age, in midlife.<sup>72</sup>

In addition, echogenicity (pixel intensity) of the tissue refers to the ability to reflect or transmit US waves in the context of surrounding tissues and can be altered in diseased states. Therefore, gray scale median (GSM) analysis has been used to quantify information about tissue composition in the arterial plaque region, with lower GSM value reflecting hypo-echoic lesions.<sup>73</sup> More complex methods, based on texture analysis, have been also used to quantify the spatial distribution of gray levels in the imaged tissue.<sup>74</sup> This type of approach could be used as a determinant of plaque vulnerability (virtual histology)<sup>75</sup>: indeed, the analysis quantifies the spatial distribution of gray levels in the imaged tissue, which, theoretically, might correspond to the relative distribution of echogenic and echolucent materials. Beyond conventional methods for echogenicity and texture estimation, which are applied on the original images, the application of a multiscale (wavelet) transform before image analysis, that can reveal information about discontinuities around single points or curves, has been shown to improve AP classification.<sup>76,77</sup>

A limitation related to plaque analysis is that scoring approaches (ie, based on counting number of plaques) may be ambiguous, due to contiguous lesions. Finally, 2D imaging measurements are affected by the imaging plane and can introduce variability into plaque size assessment.

#### *Future Development and Emerging Approaches—*

Emerging approaches include 3D-imaging that is a promising tool for plaque burden assessment,<sup>78</sup> but currently protocols are not standardized and require skilled operators. Contrast enhanced US (CEUS) can be used to investigate vulnerability (ie, rupture) of carotid atherosclerotic plaque by analyzing features such as surface, ulceration and intraplaque vascularization.<sup>16</sup> In particular, histopathological work has shown that the presence of microvessels within an atherosclerotic plaque is an indication of plaque instability.<sup>79</sup> Quantification of intraplaque neovascularization can be obtained by<sup>80</sup>: 1) visual scoring systems often reported on a 3-point scale from not visible to extensive appearance of microbubbles within the plaque; 2) quantitative assessment of intraplaque microvessels based on the time-intensity curve during microbubble

administration; 3) methods based on maximum or differential intensity projection; and 4) quantitative innovative software based on algorithms able to provide, for example, microvessel tree reconstruction or motion compensation. CEUS technique limitations include injection of a contrast agent, plaque size, challenging selection of the ROI (including only the atherosclerotic plaque and excluding the lumen and surroundings of the vessel) when using quantification software; moreover, that visual scoring is still often adopted.<sup>81</sup> found that CEUS has a high sensitivity for identifying histologic plaque rupture, while the measurement of concavity may enable the accurate detection of fibrous cap disruption. Moreover, according to Ref. [82] CEUS had superior sensitivity and diagnostic accuracy for the assessment of carotid plaque ulceration compared with Color Doppler US and improved the intrareader and inter-reader variability.

Finally, an emerging technique that is worth mentioning is photoacoustic. According to Ref. [83], Photoacoustic imaging (PAI) uses laser generated US waves to produce 3D images of soft tissues. PAI combines optical contrast with ultrasonic resolution and visualizes oxygenated and deoxygenated hemoglobin and a large range of optical agents. In US, contrast depends on the mechanical and elastic properties of the tissue but in PAI, contrast depends on the optical properties of the tissue, such as optical absorption. PAI provides an integrated platform for structural imaging including microvasculature, functional information such as blood oxygenation, blood flow, and temperature. This technique can be applied non-invasively in superficial arteries combining high ultrasound resolution and high optical tissue contrast for plaque analysis.<sup>83</sup>

*Accuracy.* Accuracy studies regarding plaque morphology analysis, mostly at the carotid level, use histology or MRI as a gold standard. US is well correlated with histopathological markers of plaque vulnerability.<sup>84</sup> Moreover, MRI has been shown to recognize hemorrhage better than US in particular compared with recognizing LRNC<sup>85</sup> and has been used as a gold standard in US-based studies of plaque morphology.

*Precision.* A recent study reported a Cohens kappa value equal to 0.70 ( $P < .001$ ) 95% CI (0.60–0.80) for inter-sonographer reproducibility of carotid plaque detection.<sup>86</sup> Mean interframe CVs for area,

GSM, un-normalized GSM and coarseness were 6.6, 11.8, 5.6, and 11.6%,<sup>87</sup> respectively. In general, performances in small plaques are significantly lower compared with larger ones, due to greater sensitivity of small plaques to manual delineation and out-of-plane motion.<sup>87</sup>

Carotid intra-plaque neovascularization parameters were tested. For quantitative parameters, ICC ranges were 0.84–0.98 and 0.68–0.96 for intra-observer and inter-observer variability, respectively.<sup>88</sup>

*Clinical impact.* APs appear with ageing and cardiovascular risk factors: whereas their prevalence in the general population is around 20%, 69.1% men and 54.2% women >75 years old showed carotid AP.<sup>89</sup> The detection of a carotid plaque of 50% or greater, or as a focal region with an IMT measurement  $\geq 1.5$  mm improves risk prediction<sup>5</sup> and its use is recommended in current ESC prevention guidelines to identify individuals at very high risk.<sup>90</sup>

*Strengths and Weaknesses*—Different US-based approaches are available, ranging from the simple plaque detection to more complex and sophisticated plaque description. For the latter, reference values based on large datasets are lacking as well as large studies regarding precision. The role that US processing can play in vulnerability assessment is still not fully demonstrated. Plaque detection is widely used in clinical practice for risk reclassification.

#### Diameter

*Vascular Characteristic*—Arterial diameter can be defined both as lumen-intima interfaces distance (internal diameter) or media-adventitia interfaces distance (external diameter).

*Technological Approach*—Diameter can be measured, similarly to IMT, on longitudinal scans with a linear US probe derived by standard B-mode, UHF B-mode, and RF data at different arterial sites (eg, carotid, radial, aorta, femoral arteries). With the introduction of automatic and semi-automatic methods, diameter assessment has become more reliable and instantaneous values, useful for distension assessment, can be obtained (Figure 7). For example, algorithms for contour tracking have been developed and a mean final result can take into account both different spatial and temporal contributions. Also for diameter estimation,

adoption of robust algorithms for processing B-mode US image sequences has shown a good agreement and comparable reproducibility with RF-based measurement.<sup>36</sup> Computerized systems assessing instantaneous diameter, especially real-time systems, are the basis for flow mediated dilation (FMD) and distension evaluations (see below). To obtain the final results, these evaluations require further computational steps besides the identification of the vessel border. Different segmentation methods are available for border localization related to IMT and diameter, as reported by Molinari et al<sup>22</sup> (eg, edge detection and gradient-based, dynamic programming, active contours (snakes)-based, Nakagami modeling, Hough transform), and can be adopted within contour tracking algorithms that follow the analyzed interfaces over time.

*Future Development and Emerging Approaches*—Emerging approaches include 3D-imaging that is a promising tool for diameter assessment.

*Accuracy.* Similar to IMT, accuracy of semiautomatic B-mode-based carotid diameter measurements has been tested for example taking an RF based system as a reference, reporting standard deviation of the difference of 0.110 mm.<sup>36</sup>

*Precision.* Repeatability data for carotid diameter are available for both RF and B-mode-based approaches. Diameter repeatability measures are also available for the abdominal aorta, femoral, popliteal, and radial arteries. Repeated measurements performed by removing and repositioning the US probe using a recent semiautomatic system yielded a CV of around 2% in CCA and a maximum CV of 4% in other sites.<sup>46</sup> Intersession variability was slightly higher for CCA (3%).<sup>62</sup>

*Clinical impact.* Large artery dilatation is known as part of the vascular ageing process, as a consequence of elastin fiber rupture and arterial remodeling. The process has been well described in the common carotid artery, where a quadratic relation with age has been shown in both sexes,<sup>35</sup> and this has also been observed in the aortic root.<sup>91</sup> Increased carotid diameter is associated with increased risk for CV events, but likely with marginal reclassification power on top of classical CV risk assessment.<sup>92</sup> Aortic root diameter measured by US predicts CV events in a general population sample.<sup>93</sup> Arterial diameter

assessment is currently used in clinical practice for aneurysm detection by manual measurement using calipers.

**Strengths and Weaknesses**—Carotid diameter can be reliably assessed by semi-automatic systems on the market. Reference values<sup>35</sup> have been provided by the scientific community at different sites, but their prognostic value for CV events is marginal. IMT and diameter can be assessed simultaneously on the same ultrasound data (Box 3).

### **Dynamic Elastic Properties: Wall Elasticity, Plaque Elasticity**

#### *Local Elasticity*

**Vascular Characteristic**—US imaging enables direct, quantitative (ie, without need of a circulatory model) assessment of arterial dynamic elastic properties.<sup>6,36</sup> The distension, or stroke change in diameter, of, for example, common carotid and common femoral arteries, as induced by the pulsatile changes in transmural pressure due to the pumping heart, is about 3–15% of vessel diameter in diastole.

**Technological Approach**—Thanks to the good temporal resolution of US equipment (typically above 25 frames/s), outputs can be evaluated by US data processing based on contour tracking techniques (Figure 7). Assuming a cylindrical geometry and a circular luminal cross-sectional section of the vessel, the cross-sectional distensibility coefficient (DC) and the cross-sectional compliance coefficient (CC) are defined respectively as relative and absolute change in lumen area ( $\Delta A$ ) induced by pulse pressure ( $\Delta P$ ) during systole. These indices can be calculated, from

Box 3. Summary statement—Vessel wall structure Intima-media thickness and diameter can be derived by RF and B-mode ultrasound data processing. A large number of studies reporting comparable repeatability for semi-automatic systems are available at different arterial sites. Simple plaque analysis with a conventional approach is limited to the presence and number of plaques. Further approaches, such as texture-based techniques or CEUS and new promising tools, such as 3D-imaging, are mainly applied at the carotid artery and needs further protocol standardization.

diameter measurements, as  $DC = (\Delta A / (A * \Delta P))$  and  $CC = (\Delta A / \Delta P)$ , where  $A$  is the diastolic cross-sectional area.<sup>94</sup> Typically  $\Delta P$  should be the local pulse pressure, as estimated for example from arterial tonometry or by integration of the distension waveform, calibrated to mean and diastolic pressure.<sup>95</sup> As an index of arterial stiffness, the opposite of elasticity, Young's elastic modulus is defined as  $(1 / (DC * h))$  taking into account the thickness of the arterial wall ( $h$ ). This estimation can be derived by US based techniques, able to perform simultaneously local in vivo measurement of IMT, used as an estimate for  $h$ , the arterial wall thickness.<sup>94</sup>

**Future Development and Emerging Approaches**—Other emerging approaches for direct local elasticity assessment include speckle-tracking/wall strain analysis.<sup>96–98</sup>

Vascular deformation patterns can be analyzed in longitudinal, radial, and circumferential directions, the last being the one typically performed. Two-dimensional speckle-tracking strain (2D strain) imaging quantifies the magnitude and rate of circumferential deformation (strain) of the arterial wall across the cardiac cycle, which provides a sensitive index of whole-artery wall stress.<sup>99</sup> Speckle-tracking software quantifies the motion of the arterial wall by identifying specific acoustic markers, speckles, in the gray-scale (or RF-mode) of a short-axis ultrasound image, which are tracked frame by frame throughout the cardiac cycle to generate strain and strain-rate curves. Peak circumferential strain (magnitude of deformation), systolic and diastolic strain rates (deformation velocity) are then calculated to provide a sensitive characterization of the dynamic elastic properties of the arterial wall.<sup>100,101</sup>

Although several studies have applied this technique to examine deformation at varying regions of the aorta,<sup>98</sup> the majority focus on circumferential 2D-strain of the CCA (figure 9 from Ref. [100]), which has been reported to be more sensitive at detecting age-related increases in CCA stiffness and more reliable than measures obtained by M-mode based approach (Figure 9).<sup>99,100,102</sup>

Other methods, based on *indirect estimation of local elasticity*, are available. If adequate temporal resolution is guaranteed,<sup>103</sup> US-derived local pulse wave velocity (PWV) estimation can provide information on the stiffness of the artery without the need to locally measure the pulse pressure with a further

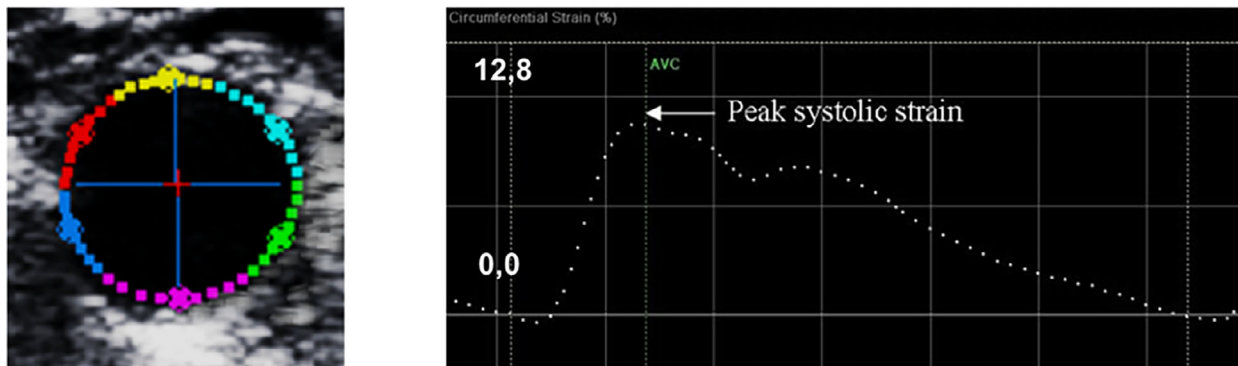
instrument. In Ref. [104], the authors, with a frame rate of 786 Hz, reported the application of linear regression to a characteristic time-point in distension waveforms in a phantom scaled according to realistic *in vivo* conditions to improve data precision. They described two approaches, threshold of 20% or the tangent method, to identify the foot of the wave to measure local PWV.<sup>104</sup> *In vivo*, a hemodynamic determinant of measurement reliability seems to be wave reflections that interfere with the distension waveform morphology.<sup>105</sup> In addition to this physiological interference with the PWV estimate, the frame-rate of about 500 Hz (ie, a 2 ms sampling interval) *in vivo* placed this particular approach at the observation limit, with expected cross-transducer ( $\sim 20$  mm) transit times 2–4 ms (corresponding to 5–10 m/s).<sup>104</sup> Less strict limitations of sampling rate are related to regional estimates of PWV<sup>106–108</sup>; as an example for regional assessment considering a distance between two sites of 0.5 m and a case of PWV around 15 m/s, the detection of a pulse transit time around 33 ms is required, so a frame rate higher than 30 fps is needed. However, these approaches remain to some degree subject to wave interference effects.

In response to temporal sampling limitations, pulse wave imaging (PWI) was introduced, using a dedicated 10-MHz linear-array transducer at an increased frame rate (1127 Hz) to estimate the velocity of the arterial wall using a 1D cross-correlation-based speckle-tracking method. The sequence of wall velocity images at different times depicts the propagation of the pulse wave in the carotid artery from the

proximal to distal sides. PWV was estimated from the spatiotemporal variation of the axial wall velocities and agreement was investigated with mechanical testing on phantoms.<sup>109</sup>

The advances in ultrafast imaging<sup>110</sup> have increased the perspectives for local estimation of PWV at accessible sites. PWV typically lies between 5 and 15 m/s and hence an adequate frame rate is required to measure pulse transit time.<sup>111</sup> The local estimation can be derived by: 1) shear wave analysis obtained by a radiation force induced in tissues by focused ultrasonic beams and a very high frame rate US imaging sequence able to capture the propagation of resulting shear waves in real time. The shear wave speed is related to tissue stiffness; 2) local PWV estimation obtained by a high frame rate imaging, generally lower than the previous one to have a better contrast that allows the use of semi-automatic tracking algorithms on longitudinal section. Under-sampling of data can be applied for a trade-off between accuracy of wall localization and computing time, and a space–time representation of the arterial wall velocity is derived. Details about accuracy and reproducibility are reported in the online supplemental Data S1. In Ref. [28], comparison between shear wave speed by elastography and local pulse wave velocity with the reference techniques carotid-femoral pulse wave velocity (via arterial tonometry) and carotid stiffness determined via echotracking was made. Based on the comparison, shear wave speed in the carotid anterior appeared to be the best candidate to evaluate arterial stiffness from ultrafast imaging.

**Figure 9.** Example of cross-sectional acquisition of the common carotid artery and extracted global circumferential strain (%) curve obtained by two-dimensional strain imaging. The artery was scanned with a 12 MHz linear probe. Adapted from “Carotid artery wall mechanics in young males with high cardiorespiratory fitness” by Pugh et al, *Exp Physiol* 2018;103:1277–1286, Copyright © Wiley.<sup>100</sup>





Reference values for clinical practice are not available yet, and a first study evaluating technical performance of *ufPWV* at the beginning and end of systole at carotid site of 201 healthy volunteers showed a sub-optimal agreement with local carotid stiffness.<sup>112</sup> Possible clinical applications of this technique are related to cardiovascular risk prediction. Compared with local carotid stiffness, it offers the advantage of being BP-independent; however, currently it requires heavy post-processing and further technological development is needed.

Finally, loop based methods<sup>113</sup> can be found in the literature. This kind of methods is based on the diameter-velocity loop and can be implemented through diameter and flow velocity measurements by B-mode and PW-Doppler analysis, respectively, avoiding the need for pressure measurement. The approach can be employed also to assess wave intensity analysis (WIA).<sup>114</sup>

*Accuracy.* As for IMT and mean diameter, RF-based echo-tracking devices have been historically adopted for measuring arterial distension.<sup>15,16</sup> Real-time computerized systems for B-mode US image sequences processing have been developed and, when using robust algorithms, they have shown a good agreement and comparable reproducibility with RF-based devices with intra-observer coefficient of variation as shown in the online supplemental Data S1.<sup>22,23</sup> The reported standard deviation of the differences are tens of  $\mu\text{m}$ , when comparing two separate acquisitions (semi-automatic RF and B-mode) by two different systems.

Some data are available also for indirect approaches. US-based carotid and aortic PWV is validated by the correlation coefficient with mechanical testing on aortic phantoms, invasive estimation, or tonometry.<sup>106,109</sup> Similarly, studies regarding carotid shear speed and loop based analysis report correlation with reference methods.<sup>28,113,115</sup>

*Precision.* Analysis by removing and repositioning the probe leads to CVs equal or lower than 11% for distension<sup>36,116</sup> whereas DC variability is higher (around 13%), due to the further variability of local pressure measurement. Indeed, the reproducibility of  $\Delta P$  is about 6–10 mmHg for >3 readings in a lab setting<sup>117</sup> and with CVs ranging within 5.1–7.9%.<sup>64</sup> Interestingly, in a study<sup>62</sup> assessing IMT, diameter, distension, CC and DC, in 10 healthy volunteers

inter- and intraobserver intra-session variabilities were comparable for all the measurements, whereas intra-observer inter-session variability resulted larger only for DC and CC. This was confirmed also in a bigger intersession variability study performed in 165 individuals showing lowest CV in diameter (CV = 1.6–1.7%), followed by CIMT (CV = 3.7–4.6%) and greater measurement variability for the functional indices (CV = DC 12.14% and CC 12.11%) where most of the variance (>80%) is explained by the subject due to variation of blood pressure.<sup>64</sup> Similarly, CVs equal or lower than 10% were obtained for circumferential strain parameters.<sup>99,100,118,119</sup>

*Clinical impact.* Local elasticity is usually measured in a plaque-free arterial segment (typically CCA). Non-linear negative relationships between age and carotid and femoral DC in both men and women were shown and age- and sex-specific reference values are available; these data were obtained from 22,708 individuals (age range 15–99 years, 54% men) for the carotid and from 5069 individuals (49.5% men, age range: 15–87 years) for the femoral artery, with both RF and B-mode based semi-automatic systems.<sup>8,35</sup> Carotid stiffness predicts CV events on top of classical CV risk factors.<sup>120</sup> Its changes over time have been used in clinical trials on cardiovascular drugs to monitor their effects.<sup>121</sup>

*Strengths and Weaknesses*—Different approaches for local assessment elasticity by ultrasound can be implemented. Direct analysis based on contour tracking techniques applied to longitudinal scans is consolidated thanks to the availability of literature about the reliability of the measurement. Generally, systems implementing this kind of measurements can simultaneously provide a structural assessment (ie, IMT and diameter) also. However, besides the assessment of the arterial instantaneous diameter, this approach requires a pulse pressure estimation. Reference values for local elasticity have been provided by the scientific community for carotid and femoral arteries and this technique can be used for improving CV risk estimation and monitor changes during treatment.

#### *Plaque Elasticity and Kinematics*

*Vascular Characteristic*—US data can be used for plaque elasticity assessment that might be adopted for clinical identification of rupture-risks, based on the

hypothesis that compressible plaque is more vulnerable and prone to rupture.

*Technological Approach*—The approach was initially developed using intravascular probes in the coronary arteries, but more recently non-invasive methods were introduced. Studies based on strain or shear wave imaging have been obtained mainly from atherosclerotic plaques in the carotid, but also the femoral and/or popliteal arteries have been investigated.<sup>122</sup>

Elastography implies the use of external sources of stress, typically the US transducer itself, which manually compresses the tissues, operates in “thumping” mode or generates shear waves. Nevertheless, an internal source of deformation (the so-called endogenous motion) in the tissue induced by heartbeat and vascular activity could be used in elasticity measurement.<sup>123,124</sup> Two main US elastography approaches can be adopted<sup>123</sup>:

1. Strain elastography (and elastography in conjunction with echogenicity estimation): The tissue strain is measured relative to the surrounding tissue and generally shown by a color-coded map. Examples of the parameters are axial strain, shear strain, and translation motion.<sup>125</sup>
2. Shear wave elastography<sup>126</sup>: this approach is based on the estimation of shear waves’ propagation resulting from an applied force (an US push pulse). An example of this approach is supersonic shear imaging that can be used to quantify Young’s modulus.

For both approaches acoustic radiation force impulse (ARFI) can be used<sup>127</sup> providing both the tissue response within the radiation force region of excitation and the speed of the shear wave propagation away from this region. Plaque characterization may be derived since higher shear wave speeds and smaller displacements may be associated with stiffer tissues, and lower shear wave speeds and larger displacements may occur with more compliant tissues. Limitations of this approach must be mentioned. Strain imaging provides only a relative estimation, and no clear consensus exists on what output strain parameters should be used. Shear wave imaging allows quantification, but optimal imaging settings should be ensured, and appropriate wave speed metrics should be chosen when attempting to

differentiate different plaque types, since the artery site can be challenging due to its size and geometry. Methods that do not require compression of the transducer and are expected to be less operator dependent are preferred in terms of accuracy/precision but might require dedicated equipment. For this reason, in addition to elastography, plaque kinematics, that is, plaque motion during the cardiac cycle, has also been investigated using ultrasound imaging (<sup>128</sup>). In particular, for carotid plaque, kinematic indices, including amplitude of tissue displacements, as well as intra-plaque movement, have been shown to be different in symptomatic and asymptomatic cases.<sup>129,130</sup>

*Accuracy.* Elastography has been compared with histology,<sup>122</sup> in differentiating between different components for plaque characterization and more specifically plaques with fibrous tissue, lipid core, intra-plaque hemorrhage and foam cells, or with other imaging modalities considered as reference techniques (MRI and CTA).<sup>131–133</sup>

*Precision.* Elastography parameters inter-frame repeatability is reported by CV (lower or equal to 16%<sup>134</sup>) or intraclass correlation coefficient between two operators (0.66–0.84).<sup>135,136</sup>

*Clinical impact.* Data about the clinical impact of this technique, which is oriented toward plaque instability detection for stroke prevention, are scarce.

*Strengths and Weaknesses*—There is still a lack of consensus and standardizations both in terms of settings and final optimal parameters, and further evidence

**Box 4. Summary statement—Dynamic elastic properties**

Direct local elasticity estimation can be derived by RF and B-mode ultrasound data processing. Studies reporting similar repeatability for semi-automatic systems are available at the carotid site; final result derives also from pressure systematic errors and variability. Indirect analysis can also be implemented and needs further investigation. Strain imaging can provide a relative estimation of plaque elasticity whereas quantification by shear wave imaging needs optimal imaging settings. Methods that do not require compression of the transducer and are expected to be less operator dependent are preferred in terms of accuracy/precision but might require dedicated equipment.

about data reliability, as well as clinical impact, are needed (Box 4).

### Reactive Vessel Properties: Flow-Mediated Dilation, Carotid Artery Reactivity, Doppler-Derived Indexes

#### Flow-Mediated Dilation

**Vascular Characteristic**—Flow-mediated dilation (FMD) is a non-invasive measure which represents an endothelium-dependent nitric (NO) mediated dilation of peripheral arteries in response to an increased blood flow and subsequent shear stress.<sup>137</sup> FMD was originally introduced in 1992<sup>138</sup> and procedures for its US-based assessment have been well established.<sup>139</sup> The measurement of FMD is based on the assessment of arterial diameter and is typically performed in the brachial artery, but it can also be done in the radial, superficial femoral, or popliteal arteries.<sup>137</sup> This endothelium-dependent dilation can be altered, by cardiovascular risk factors, relates to coronary artery endothelial function, and independently predicts cardiovascular disease outcome.<sup>137</sup>

**Technological Approach**—FMD can be assessed by processing B-mode, UHF B-mode, and RF data. The brachial artery is imaged with a linear probe (>7.5 MHz) above the antecubital fossa in the longitudinal plane with a recommended US beam angle of 60°–70°.<sup>137</sup> Baseline diameter of the examined artery is measured from 30 seconds to 1 minute. Then a sphygmomanometric cuff, placed distal to the imaged artery, is inflated for 5 minutes with pressure exceeding systolic value >50 mmHg, to occlude the arterial flow. After cuff deflation the brachial artery is imaged for at least 3 minutes: a reactive hyperemia occurs causing an increase in shear stress stimulus that induces the endothelium to release NO, a vasodilator. During the examination the position of the probe should be maintained.<sup>137</sup>

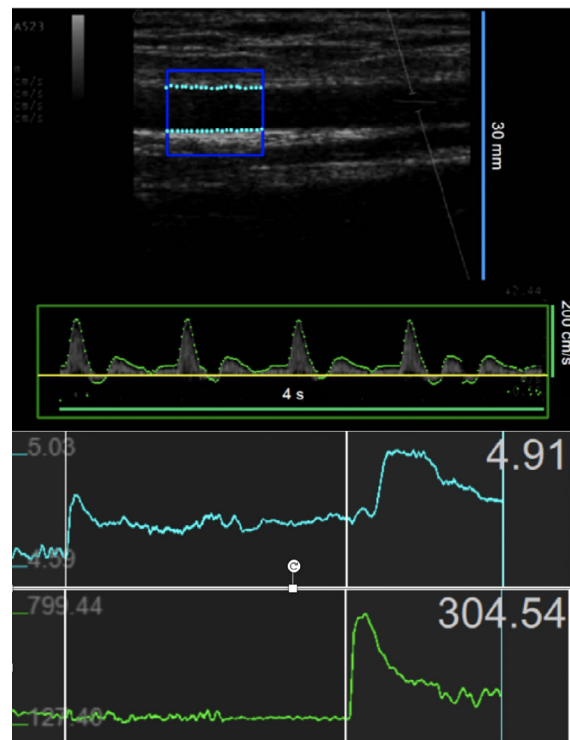
FMD is expressed as the maximum relative % change in diameter from the baseline measure after cuff deflation. Where possible, the shear stimulus is quantified during FMD responses using duplex US for simultaneous acquisition of B-mode diameter and pulsed Doppler velocity signals<sup>140</sup> (Figure 10).

Recent expert-consensus guidelines have been published with detailed insight into factors influencing the FMD measurements, related to subject-, technology-, and procedure-related factors.<sup>137,140</sup> The

importance of adhering to these guidelines has been established,<sup>10</sup> with stronger adherence to these guidelines being related to less variability of the FMD measurement.

**Future Development and Emerging Approaches**—Assessment of high-flow mediated constriction (H-FMC) and low flow-mediated constriction (L-FMC) responses has recently been proposed as a complement to FMD to better discriminate endothelial activation at baseline from true endothelial dysfunction with the combined assessment of vasodilator and vasoconstrictor capacity and their composite endpoint, the vasoactive range (VAR).<sup>141–143</sup> H-FMC response has been referred to as the slight reduction in diameter seen immediately after the release of occlusion in some subjects; for the calculation of total brachial artery reactivity, it has been suggested to use

**Figure 10.** Example of a contour tracking algorithm applied to B-mode brachial image sequences and Doppler flow velocity (top) during an FMD examination; obtained final mean diameter (mm) and shear (rate) stimulus graphs for the whole examination [ $\text{sec}^{-1}$ ] (bottom). The artery was scanned with a 10 MHz linear probe.



the minimum diameter after the release of occlusion as the alternative “baseline” diameter and this parameter has shown an association with cardiovascular diseases.<sup>144</sup> In L-FMC, the constriction response is calculated as the change from the baseline diameter of the lowest diameter during occlusion (usually monitored in around 1 minute time interval before the release of occlusion).

Regarding the probe holder, recently, a technique with automatic correction of the probe position has been developed and has shown similar results in a Japanese and a white European population.<sup>145</sup>

**Accuracy.** Accuracy of semiautomatic systems has been tested on synthetic images as percentage change of diameter<sup>146</sup>  $>(\text{error} = -0.013 + -0.069\%)$  or by comparison with already available systems<sup>147,148</sup> (negligible bias and standard deviation of the differences:  $-0.27 \pm 0.59\%$ ). Agreement with invasive coronary endothelial function has been obtained also.<sup>149</sup>

**Precision.** Manual evaluation of FMD is limited due to poor reproducibility, and should be avoided at all times.<sup>147</sup> In addition, the time of maximum vasodilation is not exactly known a priori, so that a reliable assessment of the peak response can be obtained only by continuously monitoring the artery diameter after cuff deflation. Hence, automated and semi-automated approaches have been developed. These systems can be based on wall tracking algorithms applied on RF backscattering,<sup>137</sup> or to B-mode images.<sup>146</sup>

FMD reproducibility is increased when subject-related factors (including recent physical activity, mental stress, dietary intake, smoking, alcohol, and caffeine ingestion or medication use), or air pollution<sup>150</sup> are controlled; sonographer's experience is also a key factor.<sup>10,137</sup>

Reproducibility has been estimated in three multicenter studies,<sup>33,151</sup> adopting different systems, reporting FMD intra-session coefficients of variation around 10% and slightly higher short-term (less or equal to a month) inter-session variability (CVs between 13 and 15.6%). CVs were higher for longer period between sessions and in patients rather than in controls.

**Clinical impact.** Endothelial dysfunction is considered the first step of atherosclerosis, and it is known to exacerbate with age in both sexes; age- and sex-specific reference values have been recently published.<sup>145,152</sup> Several observational longitudinal studies

demonstrated that a reduced FMD is associated with an increased risk of future cardiovascular events, both in high-risk and low-risk populations. However, its prognostic value on top of classical CV risk factors is minimal, though those conclusions are driven based on studies in which FMD reproducibility was questionable.<sup>153</sup> FMD can be modified by pharmacological and non-pharmacological treatments and may thus constitute a surrogate endpoint in cardiovascular drug trials.<sup>154</sup>

**Strengths and Weaknesses—**Guidelines for FMD assessment are available, as well as data regarding reliability of the measurement. Despite the development of semi-automatic and automatic solutions, this technique is still complex and time demanding, but may be useful in specific settings.

#### *Carotid Artery Reactivity*

**Vascular Characteristic—**Carotid artery reactivity (CAR) presents a non-invasive measure of artery function providing the percentage of carotid diameter dilation (%CAR) and blood flow velocity in response to sympathetic stimulation<sup>155,156</sup> induced by a cold-pressor test. Similar to coronary arteries,<sup>137,138</sup> sympathetic stimulation induces carotid artery dilation in healthy participants, whereas high-risk participants are more likely to demonstrate a vasoconstrictive response.

**Technological Approach—**Following 10-minutes of supine rest, carotid artery diameter and blood flow velocity are recorded using US sonography, with the probe placed 2 cm proximal to the bulb during a 1-minute baseline period. The participants then immerse their left hand (up to the wrist) in ice slush ( $\leq 4^\circ\text{C}$ ) for 3 minutes, during which the US probe position should be maintained.<sup>137,156</sup> The test is considered safe, but can be experienced as uncomfortable. Moreover, a cold-pressor test can cause hyperventilation and given end-tidal carbon dioxide is a key regulator of cerebrovascular function,<sup>157</sup> this should be controlled for by monitoring gaseous exchange when feasible. Given the risk of generalized vasospasm, patients with recent myocardial infarction are excluded. Blood pressure changes during a cold pressor test (CPT) can also confuse the interpretation.<sup>158</sup>

**Accuracy.** Accuracy has been reported as correlation with changes in left anterior descending artery velocity time integral during cold pressor test.<sup>156</sup>

**Precision.** Repeatability has been addressed for diameter, with comparable results with the above-reported literature, and for % variation, showing CVs <3% for both within and between day sessions.<sup>156</sup>

**Clinical impact.** In healthy individuals, CAR is lower with older age and in the presence of cardiovascular risk factors.<sup>156</sup> It has been demonstrated to predict risk of CV events in patients with peripheral artery disease in a single study.<sup>159</sup> The clinical impact of this technique still needs to be established.

**Strengths and Weaknesses**—This reactivity test is complex, it may be informative in specific settings; its clinical usefulness is yet to be established.

#### *Doppler-Derived Pulsatility and Resistance Index*

**Vascular Characteristic**—Hemodynamic factors such as blood flow velocity can be measured with the Doppler US technique. Moreover, two indices derived from blood flow velocity in vessels during the cardiac cycle can be obtained: resistive index (RI) introduced by Pourcelot<sup>160</sup> and pulsatility index (PI) proposed by Gosling et al<sup>161</sup> to detect peripheral vascular diseases.<sup>162</sup>

**Technological Approach**—RI and PI can be obtained in several arterial segments (the most commonly used are the carotid and renal arteries), and they are calculated as:

$$RI = \frac{(PSV - EDV)}{PSV}$$

$$PI = \frac{(PSV - EDV)}{MV}$$

where PSV and EDV are peak systolic and end diastolic velocities, respectively, and MV is the averaged mean of flow velocities over a complete cardiac cycle.<sup>163,164</sup> To measure PI a velocity curve of the entire cardiac cycle is needed, whereas RI only needs the systolic maximum and the diastolic minimum within a cardiac cycle.<sup>162</sup> Kublickas et al<sup>165</sup> demonstrated that the variability in the RI and PI for the calculation of renal flow can be reduced if 5–6 consecutive cardiac cycles are recorded.

RI and PI are commonly used for characterizing the blood flow velocity waveform recorded by Doppler ultrasonography and increase as the difference between systolic and diastolic flow velocity increases. This effect mainly depends on increased downstream flow resistance and the stiffness of the arterial wall.<sup>166,167</sup>

To calculate RI and PI in the common carotid artery (CCA) peak systolic velocity (PSV) and end diastolic velocity (EDV) are measured with the Doppler US technique usually 1–2 cm below the bifurcation with 1 mm sample in the center of carotid.<sup>164</sup>

**Accuracy.** At the renal level, RI and PI have been compared with renal histology and are associated with arteriosclerosis.<sup>168,169</sup>

**Precision.** Data about renal repeatability has been reported in terms of CVs or ICC, and resulted in CVs lower than 7% (including inter-sessions).<sup>170</sup>

**Clinical impact.** PI has been reported to be linked to downstream vascular impedance to flow<sup>171,172</sup> and RI has been found to increase in the renal artery with age and with vascular disease and risk factors.<sup>173</sup> In contrast to PI, RI has not been found reliable as an indicator of renal artery stenosis.<sup>174</sup> RI has been reported to correlate with kidney function, evaluated by serum creatinine (Kim et al 2017). In hypertensive subjects, both carotid RI and PI have been reported to correlate inversely with mean wall shear stress (WSS), a mechanical factor modulating endothelial function and vascular structure implicated in vascular remodeling and atherogenesis.<sup>164,175</sup> Renal resistive index might be useful for the early detection of renal microvascular damage and prediction of renal

**Box 5. Summary statement**—Reactive vessel properties These approaches might provide added information with respect to baseline conditions. CAR% and FMD% since derived by direct diameter measurements can be considered similarly when adopting robust semi-automatic systems. However, complexity of the protocol and maintenance of the probe position are further crucial points to be managed with respect to rest analysis. Doppler-derived indexes can be assessed at carotid and renal arteries. Further studies regarding carotid Doppler derived parameters performance might be useful.

function decline<sup>176</sup> rather than for vascular ageing assessment.

*Strengths and Weaknesses*—Though these measurements are easy and already used in clinical practice, standardization is lacking and their value as vascular ageing biomarkers needs to be clarified (Box 5).

## Discussion and Considerations for Future Developments

We conducted an extensive review of the main vascular ageing characteristics that can be derived non-invasively by US. US is a versatile and safe imaging technique that can be adopted for obtaining information related to the function, structure, and reactivity of superficial arteries. Some methodological considerations regarding resolution, accuracy, and precision evaluation of vascular characteristics obtained via US, need to be undertaken. First, resolution poses a lower limit to discriminate objects by imaging. Second, variation between repeated measurements, in general, should be lower than the smaller clinically relevant difference that has to be measured<sup>177</sup>: this is the requirement for transferring a reliable measure into clinical practice. Clinically relevant difference is established based on large longitudinal cohort studies, that is, demonstrating the cardiovascular predictive value of a biomarker. Unfortunately, those studies are not available for the vast majority of the ultrasound vascular ageing parameters. It follows that how technical performance is evaluated in the validation process is crucial. One of the aims of this article is to draw attention to the basis of measurements. The devil is in the details and knowledge of the basic principles of measurements and critical use of black box approaches are key for scientifically and ethically sound research. Since this literature review particularly focused on technical performance a limitation is that some papers showing the predictive value of an ultrasound parameter of vascular aging, might have not been included.

The usefulness of standardization in the validation process and performance metric adoption emerges in our analysis. In fact, we encountered for example a high heterogeneity in the methodology of accuracy assessment in the studies included in this

literature review. A variety of methods, with different levels of validity (correlation studies, Bland–Altman plots, comparison in terms of discrimination capabilities, measurement errors) were identified, rendering it difficult to synthesize the information. Moreover, results are often given in the sub-micron range and the expected resolution of the US system used as well as the adopted post-processing approach should consistently be reported. In our opinion, for US methods, the evaluation of agreement with a reference measurement or error estimation with phantoms (eg, silicon layer, synthetic image sequences) can be considered theoretically the most appropriate for the quantification approaches and has been widely performed for IMT, diameter and their variations. However, beyond the approach used, the real issue is the definition of the (technical) reference method, the so-called gold-standard. A general point of concern is how to validate new and better techniques. Indeed, comparison with gold standards, themselves sometimes outdated, is problematic because the new method can be much more precise but will appear discrepant from the reference. Another problem is that better resolution can introduce sources of variability when details not seen before are now visible. As reported in Ref. [178], the true quantity is rarely known in medicine and a new method is often compared with an established reference approach rather than with the real value. We can only suggest hints as to solutions to circumvent those two issues. First, putting in evidence on the closer association with hard endpoints, or known cofactors (such as age, blood pressure), provides a first argument toward better quality. Second, identifying the source of new features on images (as done, e.g., for the multiple layer signals on IMT), shows that new techniques can go beyond older ones. In this context, for example future use and developments for UHF and ultrafast US might allow an even more in-depth investigation of the blood vessel walls.

Another crucial point to be considered is the between ultrasound devices difference. Studies comparing two different versions of the same equipment are available.<sup>34,179</sup> Biases originated by model differences can be detected for example in terms of diameter and wall thickness measurements. This aspect must be taken into consideration, in particular for

longitudinal trials in which change of scanners is a natural evolution, and its impact should be tested in order to guarantee reliable output of the study.

It is worth noting that the repeatability of the reference measurement is an essential aspect in measurement quality,<sup>178</sup> especially for interventional studies. Data precision is even more important in terms of the statistical approach because it conditions the sample size calculation. Many articles reported measurements obtained by moving and repositioning the probe, and this repeatability assessment protocol is the most useful for its translation into clinical practice. Longer term repeatability comes into play for interventional studies. Robust parameters such as internal diameter of arteries are also less prone to respond to intervention than FMD, so the final calculation of sample size depends on the expected variation and its variability results in a trade-off. Sometimes, variability results from confounders. For instance, in Ref. [180] in ideal conditions (healthy controls, controlled diet, double-blind), the variability of FMD was very high within and between visits. It was shown<sup>150</sup> that 50% of the visit-to-visit variance was related to changes in air pollution, which was not anticipated. Therefore, investigating the sources of variability will always lead to improvement in measurement procedures, and to important pathophysiological findings.

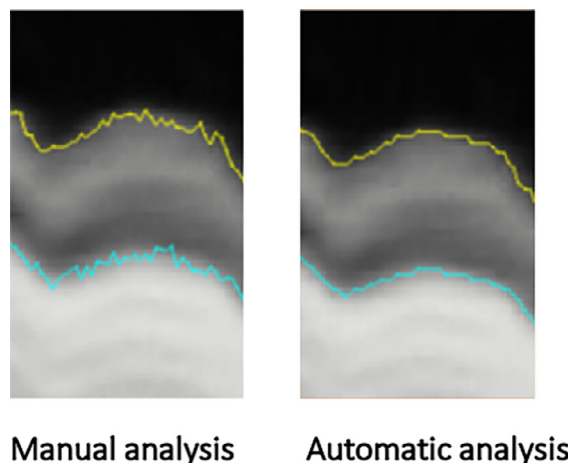
One important concern relates to calculated parameters, and propagation of error in formulas, especially if powers, multiplications, and logs are present.<sup>181</sup> Calculated parameters are relevant to ensure proper physical interpretation of the measurement; yet calculation will introduce additional noise in the estimates and may include bias and confounding. This is one of the reasons why direct measurements are preferred where possible. CCA IMT, diameter and elasticity parameters are widely published and a large body of consistent data, especially for precision analysis is available. Larger technical validation studies might provide further evidence by testing differences in measurements obtained by different methods and equipment. The adoption of semi-automatic algorithms for image processing based on a mathematical operator are particularly robust with respect to speckle noise, providing a spatial and temporal average, and working in real-time, had a key role in improving the reliability of the obtained data. The added value of the introduction of a computerized

approach has been shown in terms of improved ability to correlate with a disease, for example, coronary alterations,<sup>149,182</sup> whereas the improved ability to predict cardiovascular events with respect to manual tracings, to the best of our knowledge, has not been demonstrated yet. It is worth noting that the adoption of complex mathematical applications can also add further types of vascular analysis and advance multi-parameter approaches: this is the case, for example, of emerging methods aiming to improve quantification of complex arterial hemodynamic patterns, such as ultrasound vector flow imaging (VFI)<sup>183</sup> that can provide new insights into the interaction of blood flow and vessel properties.

As derived by the above mentioned direct measurements also CAR% and FMD% data can be considered similarly, even if standardization of the protocol and maintenance of the probe position are further crucial points to be managed with respect to rest/baseline analysis; finally, for distensibility values, we have to take into account that the final result derives also from pressure systematic errors and variability.<sup>181</sup> For some of the other emerging techniques the picture is less clear, with room for further and more robust studies about accuracy or precision.

Automatic AI-based algorithms are applied to ultrasound data for automatic structure detection and most

**Figure 11.** Example of computer-based (right) and manual (left) detection of common carotid artery echo-interfaces. Adapted from “An Automated, Interactive Analysis System for Ultrasound Sequences of the Common Carotid Artery” by Teynor et al. *Ultrasound Med Biol* 2012;38:1440–1450, Copyright © Elsevier.<sup>60</sup>



of the available studies compare their performance against a manual ground truth. As all human operators bring an unknown or variable bias, computer-based techniques should be preferred over manual measurements, if the algorithms and learning procedures are transparent and well described, and the performance indeed leads to more consistent results (an example in Figure 11 from Teynor et al<sup>60</sup>). Some caution is warranted with AI approaches, since they are not immune to “prejudice” and bias, or may not apply to specific populations<sup>184,185</sup>; training populations for AI algorithms should be sufficiently diverse, in terms of sex and ethnicity, but also different diseases. Automatic approaches might be also used for Radiomics features extraction<sup>43</sup> revealing additive vascular information. This field is still in its infancy and might provide opportunities for the role of specific estimation in clinical practice, especially when high-quality large data sets are available for testing and training of the developed method. Usability of the measurement can be improved by automatic systems that could allow a wider diffusion of non-invasive vascular ageing assessment. However, issues regarding both initial validation and performance control during the maintenance process of dynamic and ever-evolving systems are open. Standardization of acquisition and measurement procedures should be developed for clinical use of established approaches to enable both harmonized scientific basis as well as societal impact of US-supported vascular health management. Crucial points to take into consideration are bias due to the adoption of different scanners or software, whose agreement should be tested and documented,

especially in follow-up studies. Similarly, machine settings should be always reported and replicated. Moreover, identification of minimal clinical important difference, is a crucial point for drawing conclusions regarding robustness of the techniques and for the translation into practice of any biomarker: in fact, it represents the maximum allowed difference between two measurements and it is a technical requirement that the adopted techniques have to guarantee. Minimal clinical important differences must be identified by the scientific community to reach consensus about considering or not an approach suitable to detect the clinical variation that has to be monitored. Moreover, a clear identification of requirements allows implementation of validation protocols based on well-defined sample size calculation and acceptability criteria.

With the present review, the VascAgeNet authors’ group seeks to initiate more multi-disciplinary discussions with other relevant stakeholders in the vascular ageing field, toward consensus, validation guidelines, and implementation of assessment of parameters obtained via US. Besides the technological aspects described within this work, usability, compliance with regulations, and cost-effectiveness are also relevant features for sustainability and need to be taken into consideration for advancing vascular health management into practice (Box 6).

## Funding Information

This article is based upon work from COST Action CA18216 VascAgeNet, supported by COST (European Cooperation in Science and Technology, [www.cost.eu](http://www.cost.eu)). A.G. has received funding from “La Caixa” Foundation (LCF/BQ/PR22/11920008). R.E.C is supported by the National Health and Medical Research Council of Australia (reference: 2009005) and by a National Heart Foundation Future Leader Fellowship (reference: 105636). J.A. acknowledges support from the British Heart Foundation [PG/15/104/31913], the Wellcome EPSRC Centre for Medical Engineering at King’s College London [WT 203148/Z/16/Z], and the Cardiovascular MedTech Co-operative at Guy’s and St Thomas’ NHS Foundation Trust [MIC-2016-019].

### Box 6. Summary statement—Final remarks

Ultrasound is a versatile, non-invasive, and safe imaging technique that can be adopted for obtaining information about structure, elasticity, and reactivity in superficial arteries. The usefulness of standardization in the validation process and performance metric adoption emerges in our review. Computer based techniques should always be preferred to manual measures, as long as the algorithms and learning procedures are transparent and well described, and the performance leads to better results. Identification of minimal clinical important difference is a crucial point for drawing conclusions regarding robustness of the techniques and for the translation into practice of any biomarker.



## References

- Reneman RS, Meinders JM, Hoeks APG. Non-invasive ultrasound in arterial wall dynamics in humans: what have we learned and what remains to be solved. *Eur Heart J* 2005; 26:960–966. <https://doi.org/10.1093/eurheartj/ehi177>.
- Golemati S, Cokkinos DD. Recent advances in vascular ultrasound imaging technology and their clinical implications. *Ultrasonics* 2022; 119:106599. <https://doi.org/10.1016/j.ultras.2021.106599>.
- Poorthuis MHF, Halliday A, Massa MS, et al. Validation of risk prediction models to detect asymptomatic carotid stenosis. *J Am Heart Assoc* 2020; 9:e014766. <https://doi.org/10.1161/JAHA.119.014766>.
- Zamani M, Skagen K, Scott H, Russell D, Skjelland M. Advanced ultrasound methods in assessment of carotid plaque instability: a prospective multimodal study. *BMC Neurol* 2020; 20:39. <https://doi.org/10.1186/s12883-020-1620-z>.
- Peters SAE, Den Ruijter HM, Bots ML, Moons KGM. Improvements in risk stratification for the occurrence of cardiovascular disease by imaging subclinical atherosclerosis: a systematic review. *Heart* 2012; 98:177–184. <https://doi.org/10.1136/heartjnl-2011-300747>.
- Hoeks APG, Brands PJ, Smeets FAM, Reneman RS. Assessment of the distensibility of superficial arteries. *Ultrasound Med Biol* 1990; 16:121–128. [https://doi.org/10.1016/0301-5629\(90\)90139-4](https://doi.org/10.1016/0301-5629(90)90139-4).
- Engelen L, Ferreira I, Stehouwer CD, Boutouyrie P, Laurent S. Reference intervals for common carotid intima-media thickness measured with echotracking: relation with risk factors. *Eur Heart J* 2013; 34:2368–2380. <https://doi.org/10.1093/eurheartj/ehs380>.
- Bossuyt J, Engelen L, Ferreira I, et al. Reference values for local arterial stiffness. Part B: femoral artery. *J Hypertens* 2015; 33:1997–2009. <https://doi.org/10.1097/HJH.0000000000000655>.
- Olsen MH, Angell SY, Asma S, et al. A call to action and a lifecourse strategy to address the global burden of raised blood pressure on current and future generations: the lancet commission on hypertension. *Lancet* 2016; 388:2665–2712. [https://doi.org/10.1016/S0140-6736\(16\)31134-5](https://doi.org/10.1016/S0140-6736(16)31134-5).
- Greyling A, van Mil ACCM, Zock PL, Green DJ, Ghiadoni L, Thijssen DH. Adherence to guidelines strongly improves reproducibility of brachial artery flow-mediated dilation. *Atherosclerosis* 2016; 248:196–202. <https://doi.org/10.1016/j.atherosclerosis.2016.03.011>.
- Hamczyk MR, Nevado RM, Baretino A, Fuster V, Andrés V. Biological versus chronological aging: JACC focus seminar. *J Am Coll Cardiol* 2020; 75:919–930. <https://doi.org/10.1016/j.jacc.2019.11.062>.
- Bruno RM, Nilsson P, Ensgtom G, et al. 1.2 chronological versus vascular age: predictive value for cardiovascular events and identification of patients with SUPERNormal vascular aging (SUPERNOVA). *Artery Res* 2020; 25:S2. <https://doi.org/10.2991/artres.k.191224.002>.
- Climie RE, Alastruey J, Mayer CC, et al. Vascular ageing - moving from bench towards bedside. *Eur J Prev Cardiol* 2023; 4:zwad028. <https://doi.org/10.1093/eurjpc/zwad028>.
- Streiner DL, Norman GR. “Precision” and “accuracy”: two terms that are neither. *J Clin Epidemiol* 2006; 59:327–330. <https://doi.org/10.1016/j.jclinepi.2005.09.005>.
- Climie RE, Mayer CC, Bruno RM, Hametner B. Addressing the unmet needs of measuring vascular ageing in clinical practice-european cooperation in science and technology action vascagenet. *Artery Res* 2020; 26:71–75. <https://doi.org/10.2991/artres.k.200328.001>.
- Schinkel AFL, Kaspar M, Staub D. Contrast-enhanced ultrasound: clinical applications in patients with atherosclerosis. *Int J Cardiovasc Imaging* 2016; 32:35–48. <https://doi.org/10.1007/s10554-015-0713-z>.
- Anvari A, Forsberg F, Samir AE. A primer on the physical principles of tissue harmonic imaging. *Radiographics* 2015; 35:1955–1964. <https://doi.org/10.1148/rg.2015140338>.
- Entrekin RR, Porter BA, Sillesen HH, Wong AD, Cooperberg PL, Fix CH. Real-time spatial compound imaging: application to breast, vascular, and musculoskeletal ultrasound. *Semin Ultrasound CT MR* 2001; 22:50–64. [https://doi.org/10.1016/s0887-2171\(01\)90018-6](https://doi.org/10.1016/s0887-2171(01)90018-6).
- Hoeks APG, Willekes C, Boutouyrie P, Brands PJ, Willigers JM, Reneman RS. Automated detection of local artery wall thickness based on M-line signal processing. *Ultrasound Med Biol* 1997; 23:1017–1023. [https://doi.org/10.1016/S0301-5629\(97\)00119-1](https://doi.org/10.1016/S0301-5629(97)00119-1).
- Meiburger KM, Zahnd G, Fata F, et al. Carotid ultrasound boundary study (CUBS): An open multicenter analysis of computerized intima-media thickness measurement systems and their clinical impact. *Ultrasound Med Biol* 2021; 47:2442–2455. <https://doi.org/10.1016/j.ultrasmedbio.2021.03.022>.
- Meiburger KM, Acharya UR, Molinari F. Automated localization and segmentation techniques for B-mode ultrasound images: a review. *Comput Biol Med* 2018; 92:210–235. <https://doi.org/10.1016/j.combiomed.2017.11.018>.
- Molinari F, Zeng G, Suri JS. A state of the art review on intima-media thickness (IMT) measurement and wall segmentation techniques for carotid ultrasound. *Comput Methods Prog Biomed* 2010; 100:201–221. <https://doi.org/10.1016/j.cmpb.2010.04.007>.
- Suetens P. *Fundamentals of Medical Imaging*. Cambridge: Cambridge University Press; 2009.
- Hoskins PR, Martin K, Thrush A (eds). *Diagnostic Ultrasound*. Cambridge: Cambridge University Press; 2010.

25. Allan PL, Baxter GM, Weston MJ. *Clinical Ultrasound*. Elsevier Ltd; 2011.
26. Martin-McNulty B, Vincelette J, Vergona R, Sullivan ME, Wang Y-X. Noninvasive measurement of abdominal aortic aneurysms in intact mice by a high-frequency ultrasound imaging system. *Ultrasound Med Biol* 2005; 31:745–749. <https://doi.org/10.1016/j.ultrasmedbio.2005.02.012>.
27. Ming Gan L, Grönros J, Hägg U, et al. Non-invasive real-time imaging of atherosclerosis in mice using ultrasound biomicroscopy. *Atherosclerosis* 2007; 190:313–320. <https://doi.org/10.1016/j.atherosclerosis.2006.03.035>.
28. Marais L, Pernot M, Khettab H, et al. Arterial stiffness assessment by shear wave elastography and ultrafast pulse wave imaging: comparison with reference techniques in normotensives and hypertensives. *Ultrasound Med Biol* 2019; 45:758–772. <https://doi.org/10.1016/j.ultrasmedbio.2018.10.032>.
29. Rossi AC, Brands PJ, Hoeks APG. Nonlinear processing in B-mode ultrasound affects carotid diameter assessment. *Ultrasound Med Biol* 2009; 35:736–747. <https://doi.org/10.1016/j.ultrasmedbio.2008.10.011>.
30. Potter K, Reed CJ, Green DJ, Hankey GJ, Arnolda LF. Ultrasound settings significantly alter arterial lumen and wall thickness measurements. *Cardiovasc Ultrasound* 2008; 6:6. <https://doi.org/10.1186/1476-7120-6-6>.
31. Espeland MA, Craven TE, Riley WA, Corson J, Romont A, Furberg CD. Reliability of longitudinal ultrasonographic measurements of carotid intimal-medial thicknesses. *Stroke* 1996; 27:480–485. <https://doi.org/10.1161/01.STR.27.3.480>.
32. Francesconi M, Gemignani V, Gherardini R, et al. Influence of ultrasound settings on carotid biomarker assessment by B-mode image processing. *Artery Res* 2019; 25:139–144. <https://doi.org/10.2991/artres.k.191127.001>.
33. Charakida M, De Groot E, Loukogeorgakis SP, et al. Variability and reproducibility of flow-mediated dilatation in multicentre clinical trial. *Eur Heart J* 2013; 34:3501–3507. <https://doi.org/10.1093/eurheartj/ehd223>.
34. Bozec E, Girerd N, Ferreira JP, Latar I, Zannad F, Rossignol P. Reproducibility in echotracking assessment of local carotid stiffness, diameter and thickness in a population-based study (the stanislas cohort study). *Artery Res* 2020; 26:5–12. <https://doi.org/10.2991/artres.k.200314.001>.
35. Engelen L, Bossuyt J, Ferreira I, et al. Reference values for local arterial stiffness. Part A: carotid artery. *J Hypertens* 2015; 33:1981–1996. <https://doi.org/10.1097/HJH.0000000000000654>.
36. Bianchini E, Bozec E, Gemignani V, et al. Assessment of carotid stiffness and intima-media thickness from ultrasound data: comparison between two methods. *J Ultrasound Med* 2010;29:1169–1175. <https://doi.org/10.7863/jum.2010.29.8.1169>.
37. Hesamian MH, Jia W, He X, Kennedy P. Deep learning techniques for medical image segmentation: achievements and challenges. *J Digit Imaging* 2019; 32:582–596. <https://doi.org/10.1007/s10278-019-00227-x>.
38. Menchón-Lara RM, Bueno-Crespo A, Sancho-Gómez JL. Estimation of the arterial diameter in ultrasound images of the common carotid artery. In: *IWINAC 2015: Artificial Computation in Biology and Medicine*; 2015:358–367.
39. Tajbakhsh N, Shin JY, Hurst RT, et al. Automatic interpretation of carotid intima-media thickness videos using convolutional neural networks. In: *Deep Learning for Medical Image Analysis*; 2017:105–131.
40. Sudha S, Jayanthi KB, Rajasekaran C, Madian N, Sunder T. Convolutional neural network for segmentation and measurement of intima media thickness. *J Med Syst* 2018; 42:154. <https://doi.org/10.1007/s10916-018-1001-y>.
41. Menchon-Lara RM, Sancho-Gomez JL. Ultrasound image processing based on machine learning for the fully automatic evaluation of the carotid intima-media thickness. In: *2014 12th International Workshop on Content-Based Multimedia Indexing (CBMI)*.
42. Wang Y, Yao Y. Application of artificial intelligence methods in carotid artery segmentation: a review. *IEEE Access* 2023; 11:13846–13858. <https://doi.org/10.1109/ACCESS.2023.3243162>.
43. Oikonomou EK, Siddique M, Antoniadis C. Artificial intelligence in medical imaging: a radiomic guide to precision phenotyping of cardiovascular disease. *Cardiovasc Res* 2020; 116:2040–2054. <https://doi.org/10.1093/cvr/cvaa021>.
44. Touboul PJ, Hennerici MG, Meairs S, et al. Mannheim carotid intima-media thickness and plaque consensus (2004-2006-2011). *Cerebrovasc Dis* 2012; 34:290–296. <https://doi.org/10.1159/000343145>.
45. Bianchini E, Giannarelli C, Maria Bruno R, et al. Functional and structural alterations of large arteries: methodological issues. *Curr Pharm Des* 2013; 19:2390–2400. <https://doi.org/10.2174/1381612811319130007>.
46. Åstrand H, Sandgren T, Ahlgren ÅR, Länne T. Noninvasive ultrasound measurements of aortic intima-media thickness: implications for in vivo study of aortic wall stress. *J Vasc Surg* 2003; 37:1270–1276. [https://doi.org/10.1016/S0741-5214\(02\)75344-5](https://doi.org/10.1016/S0741-5214(02)75344-5).
47. Iwamoto Y, Maruhashi T, Fujii Y, et al. Intima-media thickness of brachial artery, vascular function, and cardiovascular risk factors. *Arterioscler Thromb Vasc Biol* 2012; 32:2295–2303. <https://doi.org/10.1161/ATVBAHA.112.249680>.
48. Pignoli P, Tremoli E, Poli A, Oreste P, Paoletti R. Intimal plus medial thickness of the arterial wall: a direct measurement with ultrasound imaging. *Circulation* 1986; 74:1399–1406. <https://doi.org/10.1161/01.CIR.74.6.1399>.
49. Sarkola T, Slorach C, Hui W, Bradley TJ, Redington AN, Jaeggi E. Transcutaneous very-high resolution ultrasound for the quantification of carotid arterial intima-media thickness in children - feasibility and comparison with conventional high

- resolution vascular ultrasound imaging. *Atherosclerosis* 2012; 224: 102–107. <https://doi.org/10.1016/j.atherosclerosis.2012.06.054>.
50. Mohler ER, Sibley AA, Schultz SM, Zhang L, Sehgal CM. High-frequency ultrasound for evaluation of intimal thickness. *J Am Soc Echocardiogr* 2009; 22:1129–1133. <https://doi.org/10.1016/j.echo.2009.06.021>.
  51. Dangardt F, Charakida M, Chiesa S, et al. Intimal and medial arterial changes defined by ultra-high-frequency ultrasound: response to changing risk factors in children with chronic kidney disease. *PLoS One* 2018; 13:e0198547. <https://doi.org/10.1371/journal.pone.0198547>.
  52. Sundholm JKM, Paetau A, Alböck A, Pettersson T, Sarkola T. Non-invasive vascular very-high resolution ultrasound to quantify artery intima layer thickness: validation of the four-line pattern. *Ultrasound Med Biol* 2019; 45:2010–2018. <https://doi.org/10.1016/j.ultrasmedbio.2019.04.017>.
  53. Dalla Pozza R, Pirzer R, Beyerlein A, et al. Beyond intima-media-thickness: analysis of the carotid intima-media-roughness in a paediatric population. *Atherosclerosis* 2016; 251:164–169. <https://doi.org/10.1016/j.atherosclerosis.2016.06.014>.
  54. Schmidt-Trucksäss A, Sandrock M, Cheng DC, et al. Quantitative measurement of carotid intima-media roughness - effect of age and manifest coronary artery disease. *Atherosclerosis* 2003; 166:57–65. [https://doi.org/10.1016/S0021-9150\(02\)00245-9](https://doi.org/10.1016/S0021-9150(02)00245-9).
  55. Meinders JM, Kornet L, Hoeks APG. Assessment of spatial inhomogeneities in intima media thickness along an arterial segment using its dynamic behavior. *Am J Physiol Heart Circ Physiol* 2003; 285:384–391. <https://doi.org/10.1152/ajpheart.00729.2002>.
  56. Ikeda N, Dey N, Sharma A, et al. Automated segmental-IMT measurement in thin/thick plaque with bulb presence in carotid ultrasound from multiple scanners: stroke risk assessment. *Comput Methods Prog Biomed* 2017; 141:73–81. <https://doi.org/10.1016/j.cmpb.2017.01.009>.
  57. Faïta F, Gemignani V, Bianchini E, Giannarelli C, Ghiadoni L, Demi M. Real-time measurement system for evaluation of the carotid intima-media thickness with a robust edge operator. *J Ultrasound Med* 2008; 27:1353–1361. <https://doi.org/10.7863/jum.2008.27.9.1353>.
  58. Molinari F, Liboni W, Giustetto P, Badalamenti S, Suri JS. Automatic computer-based tracings (ACT) in longitudinal 2-D ultrasound images using different scanners. *J Mech Med Biol* 2009; 9: 481–505. <https://doi.org/10.1142/S0219519409003115>.
  59. Stein JH, Korcarz CE, Mays ME, et al. A semiautomated ultrasound border detection program that facilitates clinical measurement of ultrasound carotid intima-media thickness. *J Am Soc Echocardiogr* 2005; 18:244–251. <https://doi.org/10.1016/j.jecho.2004.12.002>.
  60. Teynor A, Caviezel S, Dratva J, Künzli N, Schmidt-Trucksäss A. An automated, interactive analysis system for ultrasound sequences of the common carotid artery. *Ultrasound Med Biol* 2012; 38:1440–1450. <https://doi.org/10.1016/j.ultrasmedbio.2012.03.015>.
  61. Osika W, Dangardt F, Grönros J, et al. Increasing peripheral artery intima thickness from childhood to seniority. *Arterioscler Thromb Vasc Biol* 2007; 27:671–676. <https://doi.org/10.1161/01.ATV.0000256468.95403.6f>.
  62. Bianchini E, Corciu A, Venneri L, et al. Assessment of Cardiovascular Risk Markers from Ultrasound Images: System Reproducibility, IEEE, Bologna, Italy.
  63. Königstein K, von Schenck U, Büschges JC, et al. Carotid IMT and stiffness in the KiGGS 2 National Survey: third-generation measurement, quality algorithms and determinants of completeness. *Ultrasound Med Biol* 2021; 47:296–308. <https://doi.org/10.1016/j.ultrasmedbio.2020.10.015>.
  64. Caviezel S, Dratva J, Schaffner E, et al. Variability and reproducibility of carotid structural and functional parameters assessed with transcutaneous ultrasound - results from the SAPALDIA Cohort Study. *Atherosclerosis* 2013; 231: 448–455. <https://doi.org/10.1016/j.atherosclerosis.2013.10.010>.
  65. Sundholm J, Gustavsson T, Sarkola T. Semi-automatic border detection software for the quantification of arterial lumen, intima-media and adventitia layer thickness with very-high resolution ultrasound. *Atherosclerosis* 2014; 234:283–287. <https://doi.org/10.1016/j.atherosclerosis.2014.03.006>.
  66. Willeit P, Tschiederer L, Allara E, et al. Carotid intima-media thickness progression as surrogate marker for cardiovascular risk: meta-analysis of 119 clinical trials involving 100 667 patients. *Circulation* 2020; 142:621–642. <https://doi.org/10.1161/CIRCULATIONAHA.120.046361>.
  67. Bots ML, Groenewegen KA, Anderson TJ, et al. Common carotid intima-media thickness measurements do not improve cardiovascular risk prediction in individuals with elevated blood pressure. *Hypertension* 2014; 63:1173–1181. <https://doi.org/10.1161/HYPERTENSIONAHA.113.02683>.
  68. Den Ruijter HM, Peters SAE, Groenewegen KA, et al. Common carotid intima-media thickness does not add to Framingham risk score in individuals with diabetes mellitus: the USE-IMT initiative. *Diabetologia* 2013; 56:1494–1502. <https://doi.org/10.1007/S00125-013-2898-9>.
  69. Ferguson GG, Eliasziw M, Barr HWK, et al. The north American symptomatic carotid endarterectomy trial: surgical results in 1415 patients. *Stroke* 1999; 30:1751–1758. <https://doi.org/10.1161/01.STR.30.9.1751>.
  70. De Korte CL, Fekkes S, Nederveen AJ, Manniesing R, Hansen HRHG. Review: mechanical characterization of carotid arteries and atherosclerotic plaques. *IEEE Trans Ultrason Ferroelectr Freq Control* 2016; 63:1613–1623. <https://doi.org/10.1109/TUFFC.2016.2572260>.
  71. de Korte CL, Hansen HHG, van der Steen AFW. Vascular ultrasound for atherosclerosis imaging. *Interface Focus* 2011; 1:565–575. <https://doi.org/10.1098/rsfs.2011.0024>.

72. López-Melgar B, Fernández-Friera L, Oliva B, et al. Subclinical atherosclerosis burden by 3D ultrasound in mid-life: the PESA study. *J Am Coll Cardiol* 2017; 70:301–313. <https://doi.org/10.1016/j.jacc.2017.05.033>.
73. Johri AM, Nambi V, Naqvi TZ, et al. Recommendations for the assessment of carotid arterial plaque by ultrasound for the characterization of atherosclerosis and evaluation of cardiovascular risk: from the American Society of Echocardiography. *J Am Soc Echocardiogr* 2020; 33:917–933. <https://doi.org/10.1016/j.echo.2020.04.021>.
74. Ihnatsenka B, Boezaart AP. Ultrasound: basic understanding and learning the language. *Int J Shoulder Surg* 2010; 4:55–62. <https://doi.org/10.4103/0973-6042.76960>.
75. Golemati S, Lehareas S, Tsiaparas NN, Nikita KS, Chatziioannou A, Perrea DN. Ultrasound-image-based texture variability along the carotid artery wall in asymptomatic subjects with low and high stenosis degrees: unveiling morphological phenomena of the vulnerable tissue. *Phys Procedia* 2015; 70:1208–1211. <https://doi.org/10.1016/j.phpro.2015.08.260>.
76. Tsiaparas NN, Golemati S, Andreadis I, Stoitsis JS, Valavanis I, Nikita KS. Comparison of multiresolution features for texture classification of carotid atherosclerosis from B-mode ultrasound. *IEEE Trans Inf Technol Biomed* 2011; 15:130–137. <https://doi.org/10.1109/TITB.2010.2091511>.
77. Tsiaparas NN, Golemati S, Andreadis I, Stoitsis J, Valavanis I, Nikita KS. Assessment of carotid atherosclerosis from B-mode ultrasound images using directional multiscale texture features. *Meas Sci Technol* 2012; 23:114004. <https://doi.org/10.1088/0957-0233/23/11/114004>.
78. Baber U, Mehran R, Sartori S, et al. Prevalence, impact, and predictive value of detecting subclinical coronary and carotid atherosclerosis in asymptomatic adults: the bioimage study. *J Am Coll Cardiol* 2015; 65:1065–1074. <https://doi.org/10.1016/j.jacc.2015.01.017>.
79. Hellings WE, Peeters W, Moll FL, et al. Composition of carotid atherosclerotic plaque is associated with cardiovascular outcome: a prognostic study. *Circulation* 2010; 121:1941–1950. <https://doi.org/10.1161/CIRCULATIONAHA.109.887497>.
80. Schinkel AFL, Bosch JG, Staub D, Adam D, Feinstein SB. Contrast-enhanced ultrasound to assess carotid intraplaque neovascularization. *Ultrasound Med Biol* 2020; 46:466–478. <https://doi.org/10.1016/j.ultrasmedbio.2019.10.020>.
81. Hamada O, Sakata N, Ogata T, Shimada H, Inoue T. Contrast-enhanced ultrasonography for detecting histological carotid plaque rupture: quantitative analysis of ulcer. *Int J Stroke* 2016; 11:791–798. <https://doi.org/10.1177/1747493016641964>.
82. ten Kate GL, van Dijk AC, van den Oord SCH, et al. Usefulness of contrast-enhanced ultrasound for detection of carotid plaque ulceration in patients with symptomatic carotid atherosclerosis. *Am J Cardiol* 2013; 112:292–298. <https://doi.org/10.1016/j.amjcard.2013.03.028>.
83. Zafar H, Leahy M, Wijns W, et al. Photoacoustic cardiovascular imaging: a new technique for imaging of atherosclerosis and vulnerable plaque detection. *Biomed Phys Eng Express* 2018; 4. <https://doi.org/10.1088/2057-1976/aab640>.
84. Mitchell CC, Stein JH, Cook TD, et al. Histopathologic validation of grayscale carotid plaque characteristics related to plaque vulnerability. *Ultrasound Med Biol* 2017; 43:129–137. <https://doi.org/10.1016/j.ultrasmedbio.2016.08.011>.
85. Saba L, Agarwal N, Cau R, et al. Review of imaging biomarkers for the vulnerable carotid plaque. *JVS Vasc Sci* 2021; 2:149–158. <https://doi.org/10.1016/j.jvssci.2021.03.001>.
86. Nyman E, Vanoli D, Näslund U, Grönlund C. Inter-sonographer reproducibility of carotid ultrasound plaque detection using Mannheim consensus in subclinical atherosclerosis. *Clin Physiol Funct Imaging* 2020; 40:46–51. <https://doi.org/10.1111/cpf.12602>.
87. Stenudd I, Sjödin E, Nyman E, Wester P, Johansson E, Grönlund C. Ultrasound risk marker variability in symptomatic carotid plaque: impact on risk reclassification and association with temporal variation pattern. *Int J Cardiovasc Imaging* 2020; 36:1061–1068. <https://doi.org/10.1007/s10554-020-01801-z>.
88. Akkus Z, Hoogi A, Renaud G, et al. New quantification methods for carotid intra-plaque neovascularization using contrast-enhanced ultrasound. *Ultrasound Med Biol* 2014; 40:25–36. <https://doi.org/10.1016/j.ultrasmedbio.2013.09.010>.
89. Song P, Fang Z, Wang H, et al. Global and regional prevalence, burden, and risk factors for carotid atherosclerosis: a systematic review, meta-analysis, and modelling study. *Lancet Glob Health* 2020; 8:e721–e729. [https://doi.org/10.1016/S2214-109X\(20\)30117-0](https://doi.org/10.1016/S2214-109X(20)30117-0).
90. Visseren FLJ, Mach F, Smulders YM, et al. 2021 ESC Guidelines on cardiovascular disease prevention in clinical practice. *Eur Heart J* 2021; 42:3227–3337. <https://doi.org/10.1093/eurheartj/ehab484>.
91. Devereux RB, De Simone G, Arnett DK, et al. Normal limits in relation to age, body size and gender of two-dimensional echocardiographic aortic root dimensions in persons >15 years of age. *Am J Cardiol* 2012; 110:1189–1194. <https://doi.org/10.1016/j.amjcard.2012.05.063>.
92. Sedaghat S, van Sloten TT, Laurent S, et al. Common carotid artery diameter and risk of cardiovascular events and mortality: pooled analyses of four cohort studies. *Hypertension* 2018; 72:85–92. <https://doi.org/10.1161/HYPERTENSIONAHA.118.11253>.
93. Cuspidi C, Facchetti R, Bombelli M, et al. Aortic root diameter and risk of cardiovascular events in a general population: data from the PAMELA study. *J Hypertens* 2014; 32:1879–1887. <https://doi.org/10.1097/HJH.0000000000000264>.

94. Laurent S, Cockcroft J, Van Bortel L, et al. Expert consensus document on arterial stiffness: methodological issues and clinical applications. *Eur Heart J* 2006; 27:2588–2605. <https://doi.org/10.1093/eurheartj/ehl254>.
95. Van Bortel LM, Balkestein EJ, Van Der Heijden-Spek JJ, et al. Non-invasive assessment of local arterial pulse pressure: comparison of applanation tonometry and echo-tracking. *J Hypertens* 2001; 19:1037–1044. <https://doi.org/10.1097/00004872-200106000-00007>.
96. Lopata RGP, Nillesen MM, Hansen HHG, Gerrits IH, Thijssen JM, de Korte CL. Performance evaluation of methods for two-dimensional displacement and strain estimation using ultrasound radio frequency data. *Ultrasound Med Biol* 2009; 35: 796–812. <https://doi.org/10.1016/j.ultrasmedbio.2008.11.002>.
97. Cinthio M, Ahlgren ÅR, Bergkvist J, Jansson T, Persson HW, Lindström K. Longitudinal movements and resulting shear strain of the arterial wall. *Am J Physiol Heart Circ Physiol* 2006; 291: H394–H402. <https://doi.org/10.1152/ajpheart.00988.2005>.
98. Teixeira R, Vieira MJ, Gonçalves A, Cardim N, Gonçalves L. Ultrasonographic vascular mechanics to assess arterial stiffness: a review. *Eur Heart J Cardiovasc Imaging* 2016; 17:233–246. <https://doi.org/10.1093/EHJCI/JEV287>.
99. Bjällmark A, Lind B, Peolsson M, Shahgaldi K, Brodin LK, Nowak J. Ultrasonographic strain imaging is superior to conventional non-invasive measures of vascular stiffness in the detection of age-dependent differences in the mechanical properties of the common carotid artery. *Eur J Echocardiogr* 2010; 11:630–636. <https://doi.org/10.1093/ejehocard/jeq033>.
100. Pugh CJA, Stone KJ, Stöhr EJ, et al. Carotid artery wall mechanics in young males with high cardiorespiratory fitness. *Exp Physiol* 2018; 103:1277–1286. <https://doi.org/10.1113/EP087067>.
101. Talbot JS, Lord RN, Wakeham DJ, et al. The influence of habitual endurance exercise on carotid artery strain and strain rate in young and middle-aged men. *Exp Physiol* 2020; 105:1396–1407. <https://doi.org/10.1113/EP088384>.
102. Rosenberg AJ, Lane-Cordova AD, Wee SO, et al. Healthy aging and carotid performance: strain measures and  $\beta$ -stiffness index. *Hypertens Res* 2018; 41:748–755. <https://doi.org/10.1038/S41440-018-0065-X>.
103. Wilkinson IB, McEniery CM, Schillaci G, et al. ARTERY society guidelines for validation of non-invasive haemodynamic measurement devices: part 1, arterial pulse wave velocity. *Artery Res* 2010; 4:34–40. <https://doi.org/10.1016/j.artres.2010.03.001>.
104. Hermeling E, Reesink KD, Reneman RS, Hoeks APG. Measurement of local pulse wave velocity: effects of signal processing on precision. *Ultrasound Med Biol* 2007; 33:774–781. <https://doi.org/10.1016/j.ultrasmedbio.2006.11.018>.
105. Hermeling E, Reesink KD, Reneman RS, Hoeks APG. Confluence of incident and reflected waves interferes with systolic foot detection of the carotid artery distension waveform. *J Hypertens* 2008; 26: 2374–2380. <https://doi.org/10.1097/HJH.0B013E328311CDD5>.
106. Collette M, Palombo C, Morizzo C, Sbragi S, Kozakova M, Leftheriotis G. Carotid–femoral pulse wave velocity assessed by ultrasound: a study with echotracking technology. *Ultrasound Med Biol* 2017; 43:1187–1194. <https://doi.org/10.1016/j.ultrasmedbio.2017.02.005>.
107. Calabia J, Torguet P, Garcia M, et al. Doppler ultrasound in the measurement of pulse wave velocity: agreement with the Complior method. *Cardiovasc Ultrasound* 2011; 9:13. <https://doi.org/10.1186/1476-7120-9-13>.
108. Milan A, Zocaro G, Leone D, et al. Current assessment of pulse wave velocity: comprehensive review of validation studies. *J Hypertens* 2019; 37:1547–1557. <https://doi.org/10.1097/HJH.0000000000002081>.
109. Vappou J, Luo J, Konofagou EE. Pulse wave imaging for noninvasive and quantitative measurement of arterial stiffness in vivo. *Am J Hypertens* 2010; 23:393–398. <https://doi.org/10.1038/ajh.2009.272>.
110. Maksuti E, Widman E, Larsson D, Urban MW, Larsson M, Bjällmark A. Arterial stiffness estimation by shear wave elastography: validation in phantoms with mechanical testing. *Ultrasound Med Biol* 2016; 42:308–321. <https://doi.org/10.1016/j.ultrasmedbio.2015.08.012>.
111. Couade M. The advent of ultrafast ultrasound in vascular imaging: a review. *J Vasc Diagn Interv* 2016; 4:9. <https://doi.org/10.2147/JVD.S68045>.
112. Yang W, Wang Y, Yu Y, et al. Establishing normal reference value of carotid ultrafast pulse wave velocity and evaluating changes on coronary slow flow. *Int J Cardiovasc Imaging* 2018; 1:565–575. <https://doi.org/10.1007/s00330-018-5705-7>.
113. Segers P, Swillens A, Taelman L, Vierendeels J. Wave reflection leads to over- and underestimation of local wave speed by the PU- and QA-loop methods: theoretical basis and solution to the problem. *Physiol Meas* 2014; 35:847–861. <https://doi.org/10.1088/0967-3334/35/5/847>.
114. Di Lascio N, Kusmic C, Stea F, Fatta F. Ultrasound-based pulse wave velocity evaluation in mice. *J Vis Exp* 2017; e54362. <https://doi.org/10.3791/54362>.
115. Rabben SI, Stergiopoulos N, Hellevik LR, et al. An ultrasound-based method for determining pulse wave velocity in superficial arteries. *J Biomech* 2004; 37:1615–1622. <https://doi.org/10.1016/j.jbiomech.2003.12.031>.
116. Holtackers RJ, Spronck B, Heusinkveld MHG, et al. Head orientation should be considered in ultrasound studies on carotid artery distensibility. *J Hypertens* 2016; 34:1551–1555. <https://doi.org/10.1097/HJH.0000000000000985>.
117. Spronck B, Heusinkveld MHG, Vanmolokot FH, et al. Pressure-dependence of arterial stiffness: potential clinical implications.

- J Hypertens* 2015; 33:330–338. <https://doi.org/10.1097/HJH.0000000000000407>.
118. Yuda S, Kaneko R, Muranaka A, et al. Quantitative measurement of circumferential carotid arterial strain by two-dimensional speckle tracking imaging in healthy subjects. *Echocardiography* 2011; 28:899–906. <https://doi.org/10.1111/j.1540-8175.2011.01443.x>.
  119. Black JM, Stöhr EJ, Stone K, et al. The effect of an acute bout of resistance exercise on carotid artery strain and strain rate. *Physiol Rep* 2016; 4:e12959. <https://doi.org/10.14814/phy2.12959>.
  120. van Sloten TT, Sedaghat S, Laurent S, et al. Carotid stiffness is associated with incident stroke: a systematic review and individual participant data meta-analysis. *J Am Coll Cardiol* 2015; 66:2116–2125. <https://doi.org/10.1016/j.jacc.2015.08.888>.
  121. Tropeano A-I, Boutouyrie P, Pannier B, et al. Brachial pressure-independent reduction in carotid stiffness after long-term angiotensin-converting enzyme inhibition in diabetic hypertensives. *Hypertension* 2006; 48:80–86. <https://doi.org/10.1161/01.HYP.0000224283.76347.8c>.
  122. Mahmood B, Ewertsen C, Carlsen J, Nielsen M. Ultrasound vascular elastography as a tool for assessing atherosclerotic plaques – a systematic literature review. *Ultrasound Int Open* 2016; 02:E106–E112. <https://doi.org/10.1055/s-0042-115564>.
  123. Sigrist RMS, Liao J, El Kaffas A, Chammas MC, Willmann JK. Ultrasound elastography: review of techniques and clinical applications. *Theranostics* 2017; 7:1303–1329. <https://doi.org/10.7150/thno.18650>.
  124. Sakalauskas A, Jurkonis R, Gelman S, Lukoševičius A, Kupčinskas L. Investigation of radiofrequency ultrasound-based fibrotic tissue strain imaging method employing endogenous motion. *J Ultrasound Med* 2019; 38:2315–2327. <https://doi.org/10.1002/jum.14925>.
  125. Zhang HM, Song MM, Yang M, et al. Fast Von Mises strain imaging on ultrasound carotid vessel wall by flow driven diffusion method. *Australas Phys Eng Sci Med* 2018; 41:669–686. <https://doi.org/10.1007/s13246-018-0662-7>.
  126. Pruijssen JT, de Korte CL, Voss I, Hansen HHG. Vascular shear wave elastography in atherosclerotic arteries: a systematic review. *Ultrasound Med Biol* 2020; 46:2145–2163. <https://doi.org/10.1016/j.ultrasmedbio.2020.05.013>.
  127. Dahl JJ, Dumont DM, Allen JD, Miller EM, Trahey GE. Acoustic radiation force impulse imaging for noninvasive characterization of carotid artery atherosclerotic plaques: a feasibility study. *Ultrasound Med Biol* 2009; 35:707–716. <https://doi.org/10.1016/j.ultrasmedbio.2008.11.001>.
  128. Golemati S, Gastounioli A, Nikita K. Ultrasound-image-based cardiovascular tissue motion estimation. *IEEE Rev Biomed Eng* 2016;9:208–218.
  129. Gastounioli A, Golemati S, Stoitsis JS, Nikita KS. Carotid artery wall motion analysis from B-mode ultrasound using adaptive block matching: In silico evaluation and in vivo application. *Phys Med Biol* 2013; 58:8647–8661. <https://doi.org/10.1088/0031-9155/58/24/8647>.
  130. Golemati S, Patelaki E, Gastounioli A, Andreadis I, Liapis CD, Nikita KS. Motion synchronisation patterns of the carotid atherosclerotic plaque from B-mode ultrasound. *Sci Rep* 2020; 10:11221. <https://doi.org/10.1038/s41598-020-65340-2>.
  131. Naim C, Cloutier G, Mercure E, et al. Characterisation of carotid plaques with ultrasound elastography: feasibility and correlation with high-resolution magnetic resonance imaging. *Eur Radiol* 2013; 23:2030–2041. <https://doi.org/10.1007/s00330-013-2772-7>.
  132. Marlevi D, Mulvagh SL, Huang R, et al. Combined spatiotemporal and frequency-dependent shear wave elastography enables detection of vulnerable carotid plaques as validated by MRI. *Sci Rep* 2020; 10:403. <https://doi.org/10.1038/s41598-019-57317-7>.
  133. Di Leo N, Venturini L, de Soccio V, et al. Multiparametric ultrasound evaluation with CEUS and shear wave elastography for carotid plaque risk stratification. *J Ultrasound* 2018; 21:293–300. <https://doi.org/10.1007/s40477-018-0320-7>.
  134. Lou Z, Yang J, Tang L, et al. Shear wave elastography imaging for the features of symptomatic carotid plaques: a feasibility study: a. *J Ultrasound Med* 2017; 36:1213–1223. <https://doi.org/10.7863/ultra.16.04073>.
  135. Liu Z, Bai Z, Huang C, et al. Interoperator reproducibility of carotid elastography for identification of vulnerable atherosclerotic plaques. *IEEE Trans Ultrason Ferroelectr Freq Control* 2019; 66:505–516. <https://doi.org/10.1109/TUFFC.2018.2888479>.
  136. Ramnarine KV, Garrard JW, Dexter K, Nduwayo S, Panerai RB, Robinson TG. Shear wave elastography assessment of carotid plaque stiffness: In vitro reproducibility study. *Ultrasound Med Biol* 2014; 40:200–209. <https://doi.org/10.1016/j.ultrasmedbio.2013.09.014>.
  137. Thijssen DHJ, Bruno RM, Van Mil ACCM, et al. Expert consensus and evidence-based recommendations for the assessment of flow-mediated dilation in humans. *Eur Heart J* 2019; 40:2534–2547. <https://doi.org/10.1093/eurheartj/ehz350>.
  138. Celermajer DS, Sorensen KE, Gooch VM, et al. Non-invasive detection of endothelial dysfunction in children and adults at risk of atherosclerosis. *Lancet* 1992; 340:1111–1115. [https://doi.org/10.1016/0140-6736\(92\)93147-F](https://doi.org/10.1016/0140-6736(92)93147-F).
  139. Corretti MC, Anderson TJ, Benjamin EJ, et al. Guidelines for the ultrasound assessment of endothelial-dependent flow-mediated vasodilation of the brachial artery: a report of the international brachial artery reactivity task force. *J Am Coll Cardiol* 2002; 39:257–265. [https://doi.org/10.1016/S0735-1097\(01\)01746-6](https://doi.org/10.1016/S0735-1097(01)01746-6).
  140. Thijssen DHJ, Black MA, Pyke KE, et al. Assessment of flow-mediated dilation in humans: a methodological and physiological guideline. *Am J Physiol Heart Circ Physiol* 2011;300:H2–H12. <https://doi.org/10.1152/ajpheart.00471.2010>.

141. Gori T, Grotti S, Dragoni S, et al. Assessment of vascular function: flow-mediated constriction complements the information of flow-mediated dilatation. *Heart* 2010; 96:141–147. <https://doi.org/10.1136/HRT.2009.167213>.
142. Ostrem JD, Evanoff NG, Ryder JR, Dengel DR. Intra- and inter-day reproducibility of high-flow-mediated constriction response in young adults. *Clin Physiol Funct Imaging* 2018; 38:200–205. <https://doi.org/10.1111/CPF.12399>.
143. Humphreys RE, Green DJ, Cable NT, Thijssen DH, Dawson EA. Low-flow mediated constriction: the yin to FMD's yang? *Expert Rev Cardiovasc Ther* 2014; 12:557–564. <https://doi.org/10.1586/14779072.2014.909728>.
144. Polak JF, Ouyang P, Vaidya D. Total brachial artery reactivity and first time incident coronary heart disease events in a longitudinal cohort study: the multi-ethnic study of atherosclerosis. *PLoS One* 2019; 14:e0211726. <https://doi.org/10.1371/journal.pone.0211726>.
145. Königstein K, Wagner J, Frei M, et al. Endothelial function of healthy adults from 20 to 91 years of age: prediction of cardiovascular risk by vasoactive range. *J Hypertens* 2021; 39:1361–1369. <https://doi.org/10.1097/HJH.0000000000002798>.
146. Gemignani V, Faita F, Ghiadoni L, Poggianti E, Demi M. A system for real-time measurement of the brachial artery diameter in B-mode ultrasound images. *IEEE Trans Med Imaging* 2007; 26:393–404. <https://doi.org/10.1109/TMI.2006.891477>.
147. Sonka M, Liang W, Lauer RM. Automated analysis of brachial ultrasound image sequences: early detection of cardiovascular disease via surrogates of endothelial function. *IEEE Trans Med Imaging* 2002; 21:1271–1279. <https://doi.org/10.1109/TMI.2002.806288>.
148. Faita F, Masi S, Loukogeorgakis S, et al. Comparison of two automatic methods for the assessment of brachial artery flow-mediated dilation. *J Hypertens* 2011; 29:85–90. <https://doi.org/10.1097/HJH.0b013e32833f6938>.
149. Broxterman RM, Witman MA, Trinity JD, et al. Strong relationship between vascular function in the coronary and brachial arteries: a clinical coming of age for the updated flow-mediated dilation test? *Hypertension* 2019; 74:208–215. <https://doi.org/10.1161/HYPERTENSIONAHA.119.12881>.
150. Briet M, Collin C, Laurent S, et al. Endothelial function and chronic exposure to air pollution in normal male subjects. *Hypertension* 2007; 50:970–976. <https://doi.org/10.1161/HYPERTENSIONAHA.107.095844>.
151. Ghiadoni L, Faita F, Salvetti M, et al. Assessment of flow-mediated dilation reproducibility: a nationwide multicenter study. *J Hypertens* 2012; 30:1399–1405. <https://doi.org/10.1097/HJH.0b013e328353f222>.
152. Holder SM, Bruno RM, Shkredova DA, et al. Reference intervals for brachial artery flow-mediated dilation and the relation with cardiovascular risk factors. *Hypertension* 2021; 77:1469–1480. <https://doi.org/10.1161/hypertensionaha.120.15754>.
153. Matsuzawa Y, Kwon T-G, Lennon RJ, Lerman LO, Lerman A. Prognostic value of flow-mediated vasodilation in brachial artery and fingertip artery for cardiovascular events: a systematic review and meta-analysis. *J Am Heart Assoc* 2015; 4:e002270. <https://doi.org/10.1161/JAHA.115.002270>.
154. Lüscher TF, Taddei S, Kaski J-C, et al. Vascular effects and safety of dalcetrapib in patients with or at risk of coronary heart disease: the dal-VESSEL randomized clinical trial. *Eur Heart J* 2012; 33:857–865. <https://doi.org/10.1093/eurheartj/ehs019>.
155. Peace A, Pinna V, Timmen F, et al. Role of blood pressure in mediating carotid artery dilation in response to sympathetic stimulation in healthy, middle-aged individuals. *Am J Hypertens* 2019; 33:146–153. <https://doi.org/10.1093/ajh/hpz159>.
156. Van Mil ACCM, Hartman Y, Van Oorschoot F, et al. Correlation of carotid artery reactivity with cardiovascular risk factors and coronary artery vasodilator responses in asymptomatic, healthy volunteers. *J Hypertens* 2017; 35:1026–1034. <https://doi.org/10.1097/HJH.0000000000001274>.
157. Peebles K, Celi L, McGrattan K, Murrell C, Thomas K, Ainslie PN. Human cerebrovascular and ventilatory CO<sub>2</sub> reactivity to end-tidal, arterial and internal jugular vein PCO<sub>2</sub>. *J Physiol* 2007; 584:347–357. <https://doi.org/10.1113/jphysiol.2007.137075>.
158. Rubenfire M, Rajagopalan S, Mosca L. Carotid artery vasoreactivity in response to sympathetic stress correlates with coronary disease risk and is independent of wall thickness. *J Am Coll Cardiol* 2000; 36:2192–2197. [https://doi.org/10.1016/S0735-1097\(00\)01021-4](https://doi.org/10.1016/S0735-1097(00)01021-4).
159. van Mil ACCM, Pouwels S, Wilbrink J, Warlé MC, Thijssen DHJ. Carotid artery reactivity predicts events in peripheral arterial disease patients. *Ann Surg* 2019; 269:767–773. <https://doi.org/10.1097/SLA.0000000000002558>.
160. Pourcelot L. Indications of Doppler's ultrasonography in the study of peripheral vessels. *Rev Prat* 1975; 25:4671–4680.
161. Gosling RG, Dunbar G, King DH, et al. The quantitative analysis of occlusive peripheral arterial disease by a non-intrusive ultrasonic technique. *Angiology* 1971; 22:52–55. <https://doi.org/10.1177/000331977102200109>.
162. Petersen LJ, Petersen JR, Ladefoged SD, Mehlsen J, Jensen H. The pulsatility index and the resistive index in renal arteries in patients with hypertension and chronic renal failure. *Nephrol Dial Transplant* 1995; 10:2060–2064. <https://doi.org/10.1093/oxfordjournals.ndt.a090937>.
163. Schoning M, Walter J, Scheel P. Estimation of cerebral blood flow through color duplex sonography of the carotid and vertebral arteries in healthy adults. *Stroke* 1994; 25:17–22. <https://doi.org/10.1161/01.STR.25.1.17>.
164. Lee MY, Wu CM, Yu KH, et al. Association between wall shear stress and carotid atherosclerosis in patients with never treated essential hypertension. *Am J Hypertens* 2009; 22:705–710. <https://doi.org/10.1038/ajh.2009.77>.

165. Kublickas M, Jogestrand T, Lunell NO, Westgren M. The minimum number of cardiac cycles necessary for calculation of renal blood flow velocity indices in pregnant and non-pregnant women. *Ultrasound Obstet Gynecol* 1993; 3:31–35. <https://doi.org/10.1046/j.1469-0705.1993.03010031.x>.
166. Norris CS, Barnes RW. Renal artery flow velocity analysis: a sensitive measure of experimental and clinical renovascular resistance. *J Surg Res* 1984; 36:230–236. [https://doi.org/10.1016/0022-4804\(84\)90092-1](https://doi.org/10.1016/0022-4804(84)90092-1).
167. Ozari HO, Oktenli C, Celik S, et al. Are increased carotid artery pulsatility and resistance indexes early signs of vascular abnormalities in young obese males? *J Clin Ultrasound* 2012; 40:335–340. <https://doi.org/10.1002/jcu.21927>.
168. Gigante A, Barbano B, Di Mario F, et al. Renal parenchymal resistance in patients with biopsy proven glomerulonephritis: correlation with histological findings. *Int J Immunopathol Pharmacol* 2016; 29:469–474. <https://doi.org/10.1177/0394632016645590>.
169. Bigé N, Lévy PP, Callard P, et al. Renal arterial resistive index is associated with severe histological changes and poor renal outcome during chronic kidney disease. *BMC Nephrol* 2012; 13:1–9. <https://doi.org/10.1186/1471-2369-13-139>.
170. Dib FR, Duarte G, Sala MM, Ferriani RA, Berezowski AT. Prospective evaluation of renal artery resistance and pulsatility indices in normal pregnant women. *Ultrasound Obstet Gynecol* 2003; 22: 515–519. <https://doi.org/10.1002/uog.240>.
171. Legarth J, Thorup E. Characteristics of doppler blood-velocity waveforms in a cardiovascular in vitro model. II. The influence of peripheral resistance, perfusion pressure and blood flow. *Scand J Clin Lab Invest* 1989; 49:459–464. <https://doi.org/10.3109/00365518909089122>.
172. Bude RO, Rubin JM. Relationship between the resistive index and vascular compliance and resistance. *Radiology* 1999; 211: 411–417. <https://doi.org/10.1148/radiology.211.2.r99ma48411>.
173. Frauchiger B, Bock A, Eichlisberger R, Mihatsch MJ, Thiel G, Jäger K. The value of different resistance parameters in distinguishing biopsy-proved dysfunction of renal allografts. *Nephrol Dial Transplant* 1995; 10:527–532. <https://doi.org/10.1093/ndt/10.4.527>.
174. Veglio F, Provera E, Pinna G, et al. Renal resistive index after captopril test by Echo-Doppler in essential hypertension. *Am J Hypertens* 1992; 5:431–436. <https://doi.org/10.1093/ajh/5.7.431>.
175. Malek AM, Alper SL, Izumo S. Hemodynamic shear stress and its role in atherosclerosis. *J Am Med Assoc* 1999; 282:2035–2042. <https://doi.org/10.1001/jama.282.21.2035>.
176. Kim JH, Lee SM, Son YK, Kim SE, An WS. Resistive index as a predictor of renal progression in patients with moderate renal dysfunction regardless of angiotensin converting enzyme inhibitor or angiotensin receptor antagonist medication. *Kidney Res Clin Pract* 2017; 36:58–67. <https://doi.org/10.23876/jkrcp.2017.36.1.58>.
177. Jaeschke R, Singer J, Guyatt GH. Measurement of health status. Ascertaining the minimal clinically important difference. *Control Clin Trials* 1989; 10:407–415. [https://doi.org/10.1016/0197-2456\(89\)90005-6](https://doi.org/10.1016/0197-2456(89)90005-6).
178. Statistical methods for assessing agreement between two methods of clinical measurement – PubMed. <https://pubmed.ncbi.nlm.nih.gov/2868172/>. Accessed April 18, 2021.
179. Malik AEF, Giudici A, van der Laan KWF, et al. Detectable bias between vascular ultrasound echo-tracking systems: relevance depends on application. *J Clin Med* 2023; 12:69. <https://doi.org/10.3390/jcm12010069>.
180. Azizi M, Boutouyrie P, Bissery A, et al. Arterial and renal consequences of partial genetic deficiency in tissue kallikrein activity in humans. *J Clin Invest* 2005; 115:780–787. <https://doi.org/10.1172/jci23669>.
181. Ku HH. *Notes on the Use of Propagation of Error Formulas. Journal of Research of the National Bureau of Standards - C. Engineering and Instrumentation* 1966; 70C, October-December. 1966
182. Ikeda N, Gupta A, Dey N, et al. Improved correlation between carotid and coronary atherosclerosis SYNTAX score using automated ultrasound carotid bulb plaque IMT measurement. *Ultrasound Med Biol* 2015; 41:1247–1262. <https://doi.org/10.1016/j.ultrasmedbio.2014.12.024>.
183. Baun J. Emerging technology: ultrasound vector flow imaging—a novel approach to arterial hemodynamic quantification. *J Diagn Med Sonogr* 2021; 37:599–606. <https://doi.org/10.1177/87564793211036013>.
184. DeCamp M, Lindvall C. Latent bias and the implementation of artificial intelligence in medicine. *J Am Med Inform Assoc* 2020; 27:2020–2023. <https://doi.org/10.1093/jamia/ocaa094>.
185. Obermeyer Z, Powers B, Vogeli C, Mullainathan S. Dissecting racial bias in an algorithm used to manage the health of populations. *Science* 2019; 366:447–453. <https://doi.org/10.1126/science.aax2342>.